ADSORPTIVE REMOVAL OF PHENOL BY ACTIVATED CARBON: MODELING STUDIES

A DISSERTATION

Submitted in partial fulfillment of the
requirements for the award of the degree
of
MASTER OF TECHNOLOGY
in
CHEMICAL ENGINEERING
(With Specialization in Computer Aided Process Plant Design)

By

FAHAD ISLAM

DEPARTMENT OF CHEMICAL ENGINEERING
INDIAN INSTITUTE OF TECHNOLOGY ROORKEE
ROORKEE -247 667 (INDIA)
JUNE, 2009

CANDIDATE'S DECLARATION

I hereby declare that the work which is being presented in the dissertation entitled "**ADSORPTIVE REMOVAL OF PHENOL BY ACTIVATED CARBON: MODELING STUDIES**", in partial fulfillment of the requirement for the award of the degree of Master of Technology in Chemical Engineering with specialization in "**COMPUTER AIDED PROCESS PLANT DESIGN**", submitted in the Department of Chemical Engineering, Indian Institute of Technology Roorkee, Roorkee is an authentic record of my own work carried out during the period from July 2008 to June 2009, under the guidance of **Dr. SURENDRA KUMAR**, Professor, Department of Chemical Engineering, Indian Institute of Technology Roorkee.

The matter embodied in this dissertation work has not been submitted for the award of any other degree.

Date: 29.06.2009
Place: IIT Roorkee

(FAHAD ISLAM)

CERTIFICATE

This is to certify that the above statement made by the candidate is correct to the best of my knowledge.

29.6.09
Dr. SURENDRA KUMAR
(Professor)
Department of Chemical Engineering
Indian Institute of Technology Roorkee.

ACKNOWLEDGEMENT

I am greatly indebted to my guide **Dr. SURENDRA KUMAR** Professor, Department of Chemical Engineering, Indian Institute of Technology Roorkee, for his kind support and guidance during the entire course of this work. His cooperation and in-depth knowledge have made my work possible.

My special thanks are due to **Dr. (Mrs.) Shashi**, Assistant Professor, Department of Chemical Engineering, IIT Roorkee, whose valuable knowledge help me in understanding the phenomena during dissertation work.

I would also like to thanks my Parents without whose support I can't come up with this work in due time.

I would like to thank **Dr. I. D. Mall**, Professor and Head, Department of Chemical Engineering, IIT Roorkee and **Dr. I. M. Mishra**, Professor and Chairman, DAC, for providing various facilities during the course of this dissertation work which enabled my work to roll faster.

I would like to thank Md. Danish for his kind cooperation.

I would like to thank Z. Rahman, Ms. Tripta Garg and Mange Ram for their kind cooperation.

I would like to thank Arun, Prem, Ravindra, Jitendra and all my classmates for their suggestions and help in completion of this dissertation work.

Last but not the least I would thank my God.

Thanks are also due to CAD CENTRE facilities.

ABSTRACT

Phenol is a target pollutant to be removed from waste waters from different industries because of its toxicity. The kinetic behavior of a fixed-bed adsorber can be explained and the characteristic break through curve for the adsorption of phenol in waste water onto Activated Carbon can be obtained through mathematical models. Langmuir isotherm model is used to fit the equilibrium data. The proposed mathematical model for fixed-bed adsorption is solved by Explicit Finite difference technique followed by implementing a computer algorithm in MATLAB. And results are compared with experimental data in literature. The effects of important and influencing parameters such as flow rate, particle radius, inlet adsorbate concentration, bed height are studied.

CONTENTS

NOMENCLATURE

a_p	Radius of the adsorbent pellets, m
A	Area of cross section, m^2
b	Langmuir isotherm parameter, ml/mg
c	Solute concentration in the liquid phase inside the pores, mg/l
C_b	Bulk phase dye concentration, mg/ml
C_s	Liquid phase concentration in equilibrium with q_s on the surface, mg/ml
C_{bo}	Inlet adsorbate concentration, mg/ml
D_L	Axial dispersion coefficient, m^2/s
D_p	Pore diffusion coefficient, m^2/s
k_f	External film mass transfer coefficient, m/s
L	Column length, m
q	Average adsorbed phase dye concentration, mg/g
q_m	Maximum adsorption capacity, mg/g
q_s	Concentration on the surface of the pellet, mg/g
Q	Flow rate, ml/min
r	Radial coordinate, m
t	Time, s
V	Superficial velocity, m/s
V_o	Initial superficial velocity, m/s

V_i	Interstitial velocity inside the bed, m/s
z	Axial coordinate, m
$\overline{C}$	Dimensionless bulk phase dye concentration, (C_b / C_{bo})
Z	Dimensionless distance, (z/L)
τ	Dimensionless time, (tD_L / L^2)
$\overline{V}$	Dimensionless velocity, (V/V_o)
$\hat{C}$	Dimensionless solute concentration, (c/C_s)
η	Dimensionless radius, (r/R)
i	Index variable
j	Index variable
N	Total number of mesh points

Greek Symbols

ε	Bed porosity
ε_p	Porosity of the adsorbent pellet
ρ_l	Solution density, kg/m^3
ρ_s	Particle density, kg/m^3
ρ_p	Bed density, kg/m^3

LIST OF FIGURES

LIST OF TABLES

CHAPTER 1

INTRODUCTION

Industrial processes generate a variety of molecules that pollutes air and water. These molecules have negative impacts for ecosystems and humans (toxicity and mutagenic properties). Phenol is one of the most common organic water pollutant, because it is toxic even at low concentrations, and also its presence in natural water can lead further to the formation of substituted compounds during disinfection and oxidation processes. Phenol is also relevant in the field of environmental research, because it has been chosen frequently as a model pollutant and many data are available on its removal and destruction in particular with respect to wastewater treatments. In this review, some recent advance methods for phenol removal from fluid streams will be shortly reviewed [5]. The idea is to summarize all possible techniques to remove phenol from fluid streams, considering the most recent literature data. This work is expected to be useful to support the choice of the best technique to treat phenol emissions in practical cases.

1.1 WASTE WATER TREATMENT TECHNOLOGIES

Waste-water treatment methods are broadly classified into physical, chemical and biological processes. Some of the unit operations in each category are listed below.

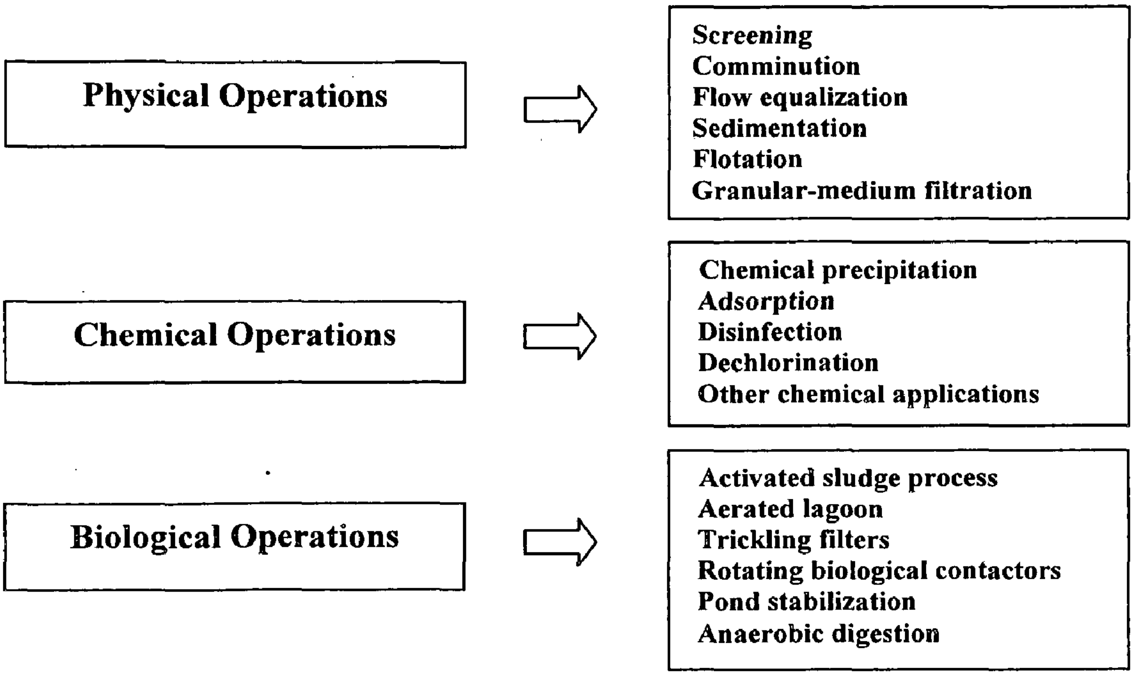

1.2 WASTE WATER CHARACTERIZATION

Waste water is characterized in terms of its physical, chemical and biological composition. The composition of industrial waste water is quiet varied, its constituents ranging from organic solvents, oils, suspended solids to dissolved chemical compounds. Many of polluting chemical substances is released by different industries [11]. Most of the chemicals are toxic, some are even suspected of cancer, some are valuable enough warrant recovery. The principal physical properties and the chemical and the biological constituents of waste water and their sources are listed in Table 1.1.

Table 1.1: Physical, chemical and biological characteristics of waste water and their sources.

Characteristic	**Source**
Physical properties	
Color	Domestic and industrial wastes
Odor	Decomposing waste water, industrial wastewaters
Solids	Domestic water supply, domestic and industrial wastes, soil erosion
Temperature	Domestic and industrial wastes
Chemical constituents	
Organic	
Carbohydrates	Domestic, commercial and industrial wastes
Fats, oils and grease	Domestic, commercial and industrial wastes
Pesticides	Agricultural wastes
Phenols	industrial wastes
Proteins	Domestic, commercial and industrial wastes
Priority pollutants	Domestic, commercial and industrial wastes
Surfactants	Domestic, commercial and industrial wastes
Volatile organic compounds	Domestic, commercial and industrial wastes
Other	Natural decay of organic materials
Inorganic	
Alkalinity	Domestic wastes, domestic water supply, ground water infiltration
Chlorides	Domestic wastes, domestic water supply, ground water infiltration

Heavy metals	Industrial wastes
Nitrogen	Domestic and agricultural wastes
pH	Domestic, commercial and industrial wastes
Phosphorous	Domestic, commercial and industrial wastes, natural run off
Priority pollutants	Domestic, commercial and industrial wastes
Sulfur	Domestic, commercial, industrial wastes, domestic water supply
Gases	
Hydrogen sulfide	Decomposition of domestic wastes
Methane	Decomposition of domestic wastes
Oxygen	Domestic water supply, surface-water infiltration
Biological constituents	
Animals	Open water course and treatment plants
Plants	Open water course and treatment plants
Eubacteria	Domestic wastes, surface-water infiltration
Archaebacteria	Domestic wastes, surface-water infiltration
Viruses	Domestic wastes

1.3 INDUSTRIAL WASTE WATER TREATMENT

Industrial facilities that send their wastes to municipal treatment plants must meet certain minimum standards to ensure that the wastes have been adequately pretreated and will not damage municipal treatment facilities. Increased number of stringent environmental laws enforces the treatment of waste water according to the norms specified by Central Pollution Control Board (CPCB). Advanced waste water treatment comprises several individual unit operations, unit processes used separately or in combination with other process to achieve very high overall treatment efficiencies (Figure 1.1). The unit operations and processes grouped together to provide various levels of treatment are as follows.

- Preliminary waste water treatment
- Primary waste water treatment
- Secondary waste water treatment
- Tertiary waste water treatment

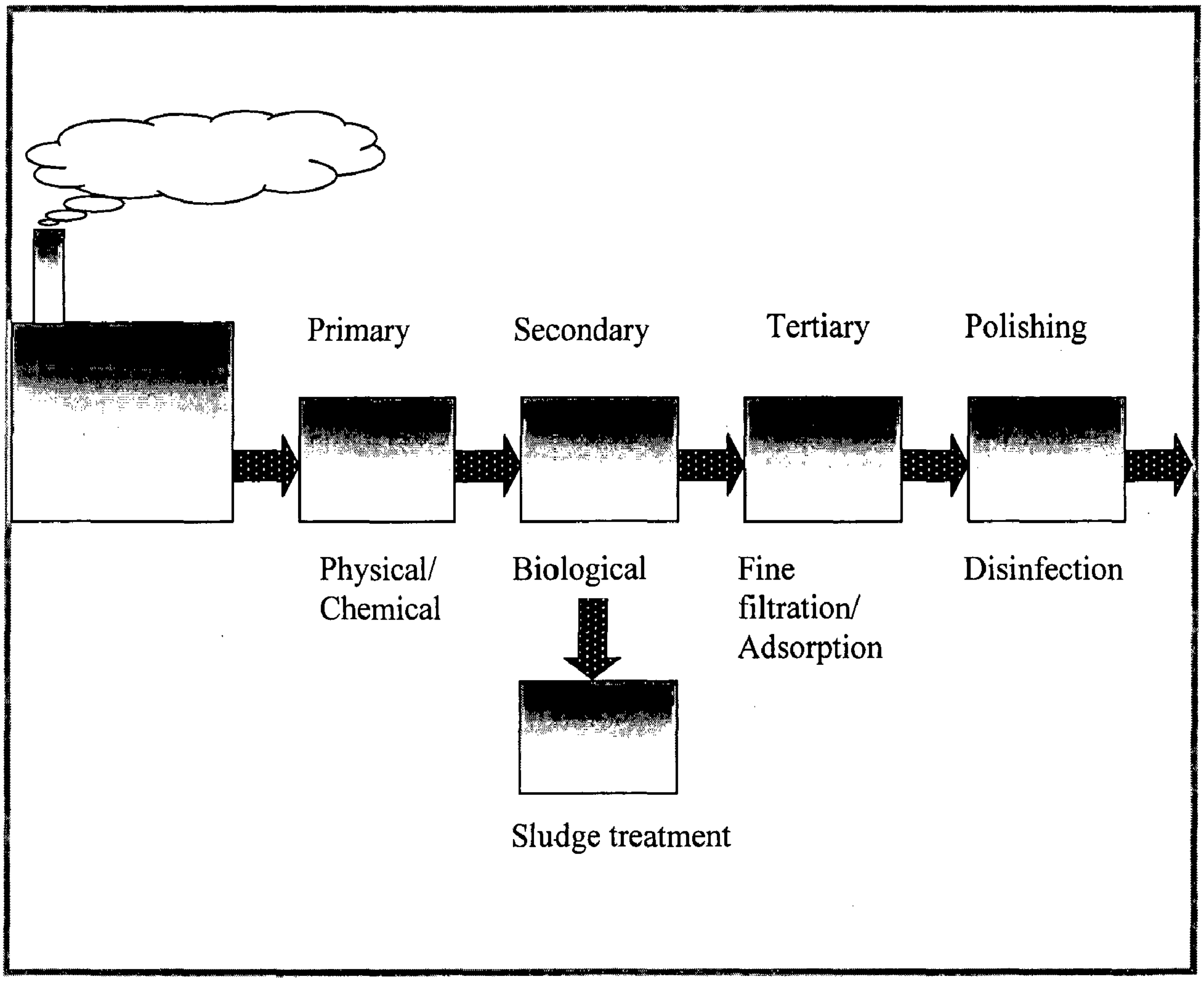

Figure 1.1: Industrial waste water treatment process.

1.4 PHENOL

Phenol is found naturally in decaying dead organic matter like rotting vegetables and in coal. It was first isolated in 1834 from coal tar and this remained the main source of phenol until the First World War. The first synthetic method was then devised and all of the phenol today is manmade. The prolonged sulphonation of benzene produces a benzene sulphonic acid, which, when fused with caustic alkalis, form a phenol.

Table 1.2: Properties of Phenol

Characteristic/Properties	Information
Chemical name	Phenol
Synonym(s)	Benzenol, hydroxylbenzene, monophenol, oxybenzene, phenyl alcohol, phenyl hydrate
Registered trade name(s)	Carbolic acid, phenic acid, phenic alcohol
Chemical formula	C_6H_6O
Chemical structure	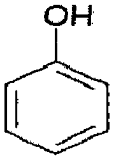
Molecular weight	94.11
Color	Colorless to light pink
Physical state	Crystalline solid liquid (w/ 8% H2O)
Melting point	43 °C
Boiling point	181.8 °C
Density at 20 °C/4 °C	1.0545 at 45 °C/4 °C
Vapor density	3.24
Odor	Distinct aromatic, somewhat sickening, sweet and acrid odor
Vapor pressure at 25 °C	0.35
Henry's law constant	4.0x10-7 m3/mol
Auto-ignition temperature	715 °C
Flashpoint, open cup	85 °C
Flashpoint, closed cup	79 °C
Flammability limits (in air, by % v)	1.7–8.6%

1.4.1 Phenol Industrial Synthesis and Sources

Currently phenol is produced at a rate of about 6 million tons/yr worldwide, with a significantly increasing trend. The so called Hock process, i.e., the three-step cumene synthesis and oxidation processes. It is simultaneous synthesis of phenol and acetone from benzene, propylene and oxygen. It produces about 95% of the phenol used in the world. These processes involve [25].

(i) Alkylation of benzene with propene to form cumene, catalyzed by phosphoric acid, aluminum chloride or, recently, by beta or MCM22 zeolite.

(ii) Oxidation of cumene to cumene hydroperoxide (CHP) with air proceeding via a free-radical mechanism that is essentially auto-catalyzed by CHP.

(iii) Cleavage of cumene hydroperoxide to phenol and acetone, catalyzed by sulphuric acid.

Several alternative industrial synthesis of phenol exist, i.e., through chlorobenzene (reaction with caustic soda at 350 °C) or by sodic benzensolfonate alkaline fusion or by oxidation of toluene via benzoic acid [7]. Phenol is also present in benzole and coal tar produced during coal coking. It may be separated from these byproducts by extraction with caustic solutions as sodium phenate.

It is shipped in the molten state at elevated temperatures or in the solid or crystalline form. It is also available as an aqueous solution. Phenol and many substituted phenols are natural components of many substances (e.g., tea, wine and smoked foods), and phenol is also emitted from the combustion of fossil fuels and tobacco. It is also present in animal wastes and decomposing organic material and may be formed in air as a product of benzene photo oxidation. Bacteria in the environment quickly break down phenol, and so levels in air (1-2 days), water (9 days) and soil (2-5 days) are generally quite low.

1.4.2 Phenol Industrial Applications

As a pure substance, phenol is used as a disinfectant, for the preparation of some cream and shaving soap for its germicidal and local anesthetic properties, in veterinary medicine as an internal antiseptic and gastric anesthetic, as a peptizing agent in glue, as an extracting solvent in refinery and lubricant production, as a blocking agent for blocked isocyanate monomers, as a reagent in chemical analysis and as a primary petrochemical intermediate. Various aromatic compounds (mainly phenol and its derivatives) are raw materials and/or basic products of the chemical industry. As a result, they are widely found in the effluents of these industries or reach the surface or ground water via use by consumers. These are very toxic to the flora and fauna, are not readily biodegradable and therefore, pose environmental problems [12]. Its largest use (35%) is to produce phenolic resins like phenol-formaldehyde resins (Bakelite) which are low-cost thermosetting resins applied as plywood adhesive, construction, automotive and appliance industries. By reaction with acetone it may also be converted into bisphenol A, a monomer for epoxy-resins (28%). It is also used to produce cyclohexanone and cyclohexanone-cyclohexanol mixtures by selective catalytic hydrogenation. Cyclohexanone is later converted into its oxime and further to ε-caprolactame, the monomer for nylon-6 (16% of phenol applications). The mixture cyclohexanone-cyclohexanol is oxidized by nitric acid to adipic acid, one of the monomers for the production of nylon-66. Phenol is also used to produce polyphenoxy and polysulphone polymers, corrosion-resistant polyester and polyester polyols.

Phenol may be converted into xylenols, alkylphenols, chlorophenols, aniline, and other secondary intermediates in the production of surfactants, fertilizers, explosives, paints and paint removers, textiles, rubber and plastic plasticizers and antioxidants, and curing agents and so on. Phenol is also a building block for the synthesis of pharmaceuticals, such as, e.g. aspirin.

1.4.3 Health Hazards

The sterilizing activity of phenol was discovered by the English surgeon Joseph Lister in 1865. The germicidal activity of phenol appears associated to its protein denaturing ability. It has lipofile properties, so it binds itself to the batteric protein by hydrogen bonds. On the other hand, phenol has relevant health effects for humans. The manufacture and transportation of phenol as well as its many uses may lead to worker exposures to this substance, through inhalation, ingestion, eye or skin contact, and absorption through the skin. Phenol is rapidly absorbed through the skin and can cause skin and eye burns upon contact. Comas, convulsions, cyanosis and death can result from overexposure to it. Internally, phenol affects the liver, kidneys, lungs, and vascular system. The ingestion of 1 g of phenol is deadly for man.

During Second World War Nazi used phenol toxicity for refining extermination techniques, making phenol injections for killing the prisoners. Death was coming up in a few seconds and the method was considered to efficacious and economic [5]. No evidence exists to indicate that phenol has any carcinogenic potential.

1.5 ADSORPTION

A separation process in which solids are used for the removal of substances from either gaseous or liquid solutions is known as adsorption. It involves nothing more than the preferential partitioning of substances from the gaseous or liquid phase onto the surface of a solid substrate. The process of adsorption involves separation of a substance from one phase accompanied by its accumulation or concentration at the surface of another. The adsorbing phase is the adsorbent, and the material concentrated or adsorbed at the surface of that phase is the adsorbate.

Two key parameters:

- Amount of the surface area. The more the merrier.
- "Residence time" of fluid within adsorbing media.

Examples:

- Decolorization of sugar solutions using charcoal.
- Solids such as activated carbon and synthetic resins are used widely in industrial applications and for purification of water and wastewater.

1.5.1 Types of Adsorption

There are two types of adsorption.

- Physical adsorption
- Chemisorption

Physical adsorption:

A reversible phenomena, is the result of vanderwaals forces and electrostatic forces between adsorbate molecules and the atoms which compose the adsorbent surface. The adsorbed substance penetrates with in crystal lattice of the solid and does not dissolve in it but remains entirely upon the surface. In industrial operations the types we shall consider depend upon the reversibility of adsorption for recovery of adsorbent for reuse, for the recovery of adsorbed substances, or for the fractionation of mixtures.

Chemisorption:

An adsorption phenomenon is a result of chemical interactions between solid and adsorbed substance. The strength of chemical bond may vary considerably and identifiable chemical compounds in the usual sense may not actual form, but the adhesive force is generally much greater than that found in physical adsorption. The heat liberated is usually large and is of the order of the heat of chemical reaction. The process is frequently irreversible and on desorption of the original substance will often be found to have undergone a chemical change [28].

The same substance which under the conditions of low temperature will undergo substantially only physical adsorption upon a solid will sometimes exhibits chemisorption at higher temperatures, and both phenomena may occur simultaneously.

1.5.2 Adsorbents

The solid surface on which the adsorbate is going to be adsorbed is called adsorbent. The adsorbents are characterized first by surface properties such as surface area and polarity. A large specific surface area is preferable for providing large adsorption capacity, but the creation of a large internal surface area in a limited volume inevitably gives rise to large numbers of small sized pores between adsorption surfaces. A Adsorbents are mostly micro porous, high specific surface material's (200 - 2000 m^2/g) The size of the micro pores determines the accessibility of adsorbate molecules to the internal adsorption surface, so the pore size distribution of micro pores is another important property for characterizing adsorptivity of adsorbents. Especially materials such as zeolite and carbon molecular sieves can be specifically engineered with precise pore size distributions and hence tuned for a particular separation.

Surface polarity corresponds to affinity with polar substances such as water or alcohols. Polar adsorbents are thus called "hydrophilic" and aluminosilicates such as zeolites, porous alumina, silica gel or silica-alumina are examples of adsorbents of this type. On the other hand, non polar adsorbents are generally "hydrophobic". Carbonaceous adsorbents, polymer adsorbents and silicalite are typical non polar adsorbents. These adsorbents have more affinity with oil or hydrocarbons than water. If the solid is highly porous, containing many fine capillaries, the adsorbed substance will penetrate these interstices if it wets the solid.

- ***Nature***

Adsorbent solids are usually used in granular form, varying size from 12mm in diameter to as small as 50µm. The solids must possess certain engineering properties depending on the application to which they are put. For example in the fixed bed adsorption in which liquids or gas is to flow they must not offer too great pressure drop for flow nor must they easily carried away by flowing stream. They must have adequate strength and hardness so as not to be reduced in size during handling or crushed in supporting their own weights of beds of required thickness.

- ***Physical adsorbents***

The most commonly used adsorbents are alumina, silica gel, zeolite molecular sieves, highly specific, single pore size may be fine-tuned: cations + structure type of organo-modified materials, mordenite, other natural zeolites silicalites, active carbon, Carbon molecular sieves (narrow pore distribution), impregnated carbons clays (natural and pillared clays) resins, polymers (biological, ions, large molecules) carbon nano tubes.

Activated carbon: is the trade name for a carbonaceous adsorbent which is defined as follows: Activated carbons are non-hazardous, processed, carbonaceous products, having a porous structure and a large internal surface area. These materials can adsorb a wide variety of substances, i.e. they are able to attract molecules to their internal surface, and are therefore called adsorbents.

Fuller's earth: are natural clays chiefly magnesium aluminum silicates in the form of minerals attapulgite and montomorrillonite. The clays are particularly useful in decolorizing, neutralizing, and drying. By washing and burning the adsorbed organic matter accumulating upon the clay during use, the adsorbent can be reused many times.

Activated clays: is bentonite or other clays which show essentially no adsorptive ability unless activated by treatment with sulfuric or hydrochloric acid. It is particularly useful for decolorizing petroleum products and is ordinarily discarded after a single application..

Bauxite: is a certain form of naturally occurring hydrated alumina which must be activated by heating to temperatures varying from 230 to 815°C in order to develop its adsorptive ability.

Alumina: is a hard, hydrated aluminum oxide which is activated by heating to drive off the moisture. The porous product is available as a granules or powders, used as a desiccant for gases and liquids. It can be reactivated for reuse.

Synthetic polymeric adsorbents: are porous spherical beads, 0.5mm diameter, and each bed of collection of micro spheres 10^{-4}mm diameter. The material is synthetic, made from polymerizable monomers of two major types [28]. Those made from unsaturated aromatics such as styrene and vinyl benzene are useful for adsorbing nonpolar organics from aqueous solution .Those made from acrylic esters are suitable for more polar solutes. They are used principally for treating water solutions and are regenerated by leaching with low molecular weight alcohols or ketones.

Silica gel: is a hard, granular, very porous product made from the gel precipitated by acid treatment of sodium silicate solution. It is revivified for reuse by evaporation of the adsorbed matter.

Molecular sieves: are porous, synthetic zeolite crystals, metal aluminosilicates. The "cages" of the crystal cells can entrap adsorbed matter, and the diameter of the passage ways, controlled by the crystal composition, regulates the size of the molecules which can enter. They are used for dehydration of gases and liquids, separation of gas and liquid hydrocarbon mixtures, and in a great variety of processes. They are regenerated by heating or elution [28].

1.6 ACTIVATED CARBON ADSORPTION

Organic contaminants from industrial waste streams that seriously affect human health and environment .Activated carbon are widely used for removing organic pollutants from water. The porous nature of this adsorbent material and its high surface area are suitable properties for adsorption. The volume of pores of the activated carbons is generally greater than 0.2 ml/g. The internal surface area is generally greater than $400m^2/g$. The width of the pores ranges from 0.3 to several thousand nm (Figure 1.2).

All activated carbons are characterized by their ramified pore system within which various meso pores (r = 1-25 nm), micro pores (r = 0.4-1.0 nm) and sub micro pores (r < 0.4 nm) branch off from what we call macro pores (r >25 nm).

Specific surface area is 500 to 1500 m^2/g. It offers strong adsorption power it mainly comes from Vander Walls forces.

1.6.1 Types and Features of Activated Carbon

There are many types of activated carbon. Therefore it is necessary to select one among them according to objective. The main raw materials are coal, wood, coconuts and petroleum pitch. Properties are generally depending upon activation conditions when making them from raw materials. Activation is done using high temperature steam of about 900^0 C. In case of wooden raw material, it is carbonized after soaking in chemicals such as zinc chloride. Activated carbon is divided into two types, namely powder and granules the powder cannot be easily regenerated and is usually discarded after use [10]. The granular type is generally used in waste water treatment because of continuous use, easy handling and repeated regeneration. It comes from crushing or sintering but crushed carbon is ordinarily used.

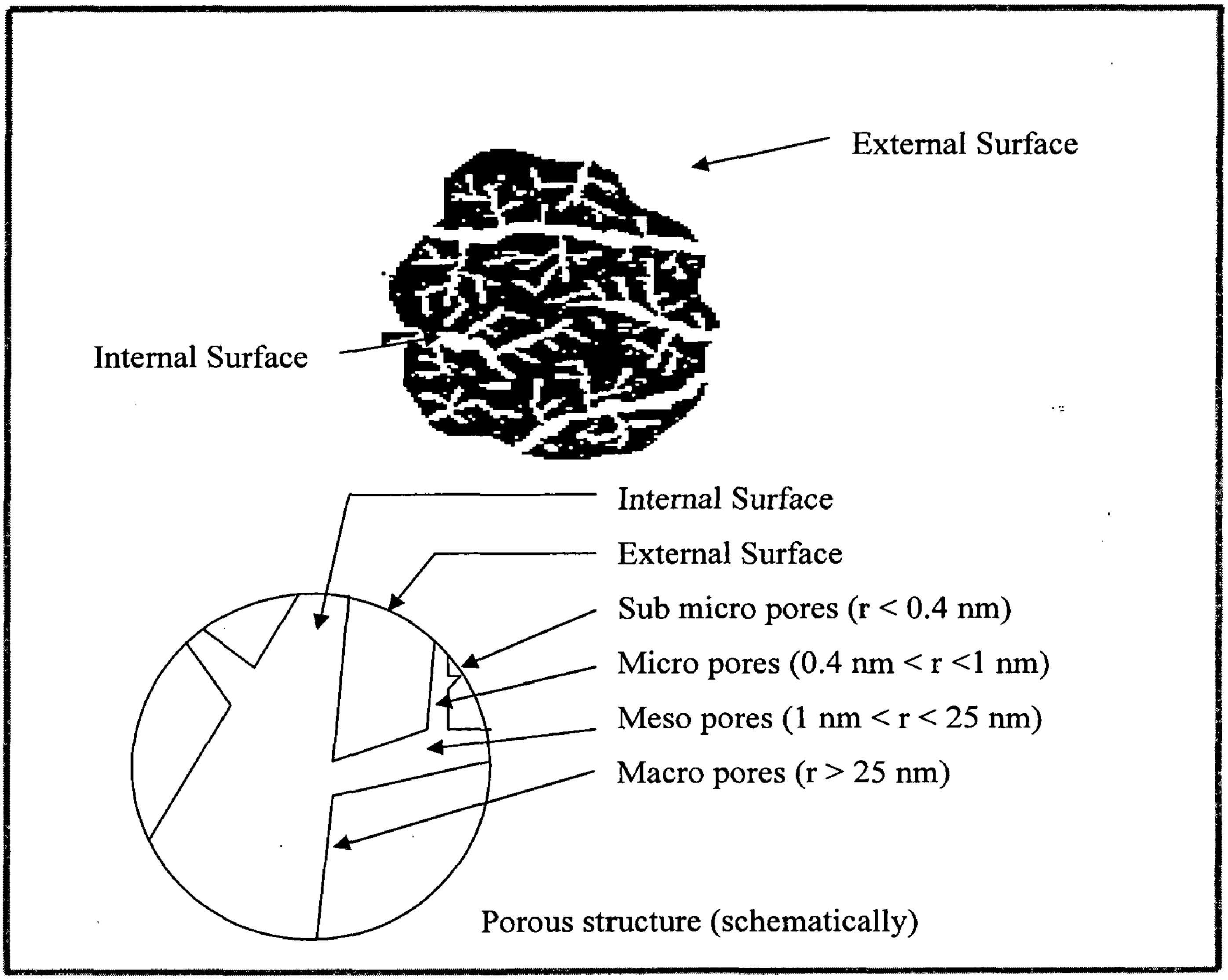

Figure 1.2: Schematic activated carbon model.

1.6.2 Factors Contributing to Activated Carbon Adsorption

Activated carbon has the following tendencies in general.

1. *Solubility*: It is hydrophobic Therefore it readily adsorbs hydrophobic substances. In aliphatic compounds, the longer the alkyl group, the more hydrophobic it is .it does not readily dissolve in water. So adsorption amount of it increases.
2. *Size of the molecule*: In general the larger the molecular weight, the larger is the adsorption amount. However, molecular diffusion velocity in the pores is slow when molecular weight is large. Therefore it may be effective to decrease molecular weight to some extent, by biological decomposition or oxidation by ozone prior to adsorption.
3. *pH*: Removal rate of organic substances can be improved by decreasing the pH of waste water to about 2 to3 .Because ionization rate organic substances in waste water is low at low pH range like this.
4. *Concentration*: In general, as the concentration of organic substances in the waste water increases, adsorption amount increases too. However, in the case of chemical substances such as surface active agents, adsorption amount is constant regardless of concentration.
5. *Water temperatures*: Unlike gas phase water temperature has less effect on adsorption in ordinary waste water.

1.7 ADSORPTION EQUILIBRIA

The great bulk of experimental data pertaining to the adsorption represents equilibrium measurements. The apparent adsorption of given solute depends on temperature, the solvent, and the type of adsorbent. The extent of adsorption of a given solute practically always decreases at increased temperature and usually greater the solubility in the solvent. It is usually reversible, so that the same isotherm results whether solute is adsorbed or desorbed.

Adsorption Isotherm

It shows the equilibrium relation between sorbent and sorbate. These are described by sorption isotherms, the ratio between the amount sorbed and that remaining in the solution at a fixed temperature at equilibrium. It takes equilibrium concentration as the axis of ordinate and the weight of solute adsorbed per unit weight of adsorbent as the axis of abscissa. The equilibrium sorption isotherm is crucial is fundamentally very crucial in design of sorption system. The adsorption isotherms described by different isotherm models

- Langmuir Isotherm
- Freundlich Isotherm
- Redlich-Peterson Isotherm
- Linear Sorption Isotherm.
- Tooth Isotherm
- Radke-Prausnitz
- Fritz-Schlunder Isotherm
- Temkin Isotherm
- Brunauer-Emmett-Teller Isotherm

Langmuir Isotherm: The Langmuir sorption isotherm has been widely applied to many pollutants sorption process [12]. It has produced good agreement with a wide variety of experimental data for the sorption of a solute from a liquid solution.

A basic assumption of the Langmuir theory is that the sorption takes place at specific homogeneous sites in the sorbent. Moreover, when a site is occupied by a solute, no further sorption can take place at that site. It has the form of

$$S_e = \frac{K_L S_m C_e}{1 + K_L C_e} \qquad (1.1)$$

where S_e is the amount adsorbed on solid at equilibrium (mg/kg), C_e is the equilibrium liquid concentration (mg/L), S_m is the adsorption capacity or adsorption maximum (mg/kg), and K_L is the adsorption intensity or Langmuir coefficient (L/mg). Equation (1.1) can be rearranged to the following linear form:

$$\frac{C_e}{S_e} = \frac{1}{K_L S_m} + \frac{C_e}{S_m} \tag{1.2}$$

Freundlich Isotherm: If the concentration of solution at equilibrium, C_e, was increased to the power of 1/n, the amount of solute sorbed being S_e, then the $C_e^{1/n} / S_e$ was a constant at a fixed temperature [2]. This experimental model can be applied to non ideal sorption on heterogeneous surfaces as well as multi-layer sorption and is expressed by the following equation:

$$S_e = K_F C_e^a \tag{1.3}$$

Assumption: An exponentially decaying sorption site energy distribution. This equation can be rearranged in the linear form by taking the logarithm of both sides as

$$\log S_e = \log K_F + a \log C_e \tag{1.4}$$

The Freundlich constant ‘a’ is a measure of deviation from adsorption linearity. If a is equal to unity the adsorption is proved to be linear, which means that adsorption sites are homogeneous or these sites of the adsorbent are not limiting in quantity and are not modified by the adsorption process itself. If ‘a’ is less than unity, this implies that increased adsorption modifies the adsorbent, giving rise to an increase in the adsorption capacity, such as forming new adsorption sites on the adsorbent surface. If ‘a’ is greater than unity the adsorption bond becomes weak, and the S_e changes significantly, with small changes in C_e.

Redlich-Peterson Isotherm: It has three parameters and incorporates the features of both the Langmuir and Freundlich equation [12]. It has a linear dependence on concentration in the numerator and an exponential function in the denominator. It can be described as follows:

$$S_e = \frac{AC_e}{1 + BC_e^g} \tag{1.5}$$

where A, B and g ($0 < g < 1$) are the isotherm constants. At low concentrations, it approximates to Henry’s law and at high concentrations its behavior approaches that of the Freundlich isotherm. It has two limiting case that can be summarized:

$$S_e = \frac{AC_e}{1 + BC_e} \tag{1.6}$$

where g = 1, i.e. the Langmuir form results.

$$S_e = \frac{AC_e}{1+B} \tag{1.7}$$

where g = 0, i.e. the Henry's law form results. Although a linear analysis is not possible for a three-parameter isotherm, a trial and error procedure has previously been applied to a pseudo-linear form of Redlich-Peterson isotherm to obtain values for the isotherm constants. Equation (1.5) can be converted to a pseudo-linear form by taking logarithms:

$$\ln\left(A\frac{C_e}{S_e}-1\right) = g\ln(C_e)+\ln(B) \tag{1.8}$$

This method involves varying the isotherm parameter, A, to obtain the maximum value of correlation coefficient for the linear regression of in (C_e) against $\ln\left(\mathrm{A}\ (C_e/S)\ -1\right)$.

Linear Sorption Isotherm: The sorption of Non Organic Compounds (NOCs) to an organic rich substrate can obey a linear sorption isotherm or Henry's equation with the following form:

$$C_s = K_d C_w \tag{1.9}$$

where C_s is the amount of solute sorbed (mg/kg), C_w the equilibrium aqueous solute concentration (mg/L), and K_d is the linear sorption coefficient. K_d is related to f_{oc}, the fractional organic carbon content of the sorbent, and K_{oc} the organic carbon-based partition coefficient of the NOC, by the following equation:

$$K_d = K_{oc} f_{oc} \tag{1.10}$$

For a certain NOC, K_{oc} is reasonably constant and thus K_d increases linearly with respect to f_{oc}. In a partitioning process, the NOC distributes itself between two immiscible phases. The partition coefficient K_{oc} reflects the ratio of NOC concentrations in the organic phase (C_{oc}) and the aqueous phase (C_w):

$$K_{oc} = \frac{C_{oc}}{C_w} \tag{1.11}$$

Since f_{oc} is dimensionless and K_{oc} has the same unit as K_d, C_{oc} has the unit of (mass of NOC) / (mass of bound organic carbon).

Toth isotherm [12]:

$$q_e = q_e^{\infty} C_e / [a + C_e^{th}]^{1/th} \tag{1.12}$$

***Radke-Prausnitz isotherm*:**

$$1/q_e = 1/KC_e + 1/KC_e^{1/p} \tag{1.13}$$

Fritz-Schlunder isotherm [12]:

$$q_e = \alpha_1 C_e^{\beta 1} / \left(1 + \alpha_2 C_e^{\beta 2}\right) \tag{1.14}$$

Brunauer-Emmett-Teller isotherm:

$$\frac{p/p_o}{q(1-p/p_o)} = \frac{1}{q_m C} + \frac{p(C-1)}{p_o q_m C} \tag{1.15}$$

***Temkin isotherm*:**

$$q_e = \frac{RT}{b}\ln(K_T C_e) \tag{1.16}$$

where

q_e	Amount of adsorbate adsorbed at equilibrium, mg/g
q_e^{∞}	Monolayer adsorption capacity parameter, mg/g
C_e	Concentration of adsorbate adsorbed at equilibrium, mg/l

1.8 ADSORPTION COLUMNS

There are mainly three kinds of equipments, namely fixed bed adsorption column, moving bed adsorption column and fluidized column. It is necessary to remove suspended solids as pretreatment regardless of type of tower.

1.8.1 Fluidized bed adsorption column

A multi stage fluidized bed adsorption tower is introduced. There are multiple stages partitioned by perforated plates in a tower (Figure 1.3). There are many nozzles on perforated plates.

Perforated plate has a structure so that activated carbon does not fall to lower stages because of the angle of repose when water flow is off. This makes it possible to run and stop raw waste water pump. New activated carbon is loaded into a weighing tank and fed by treated water to the top of tower under pumping force.

The raw waste water is fed from the bottom of the tower and moves towards the top through perforated plates. When the waste water contact with the fluidized activated carbon, organic substances get adsorbed in it. When water feed is stopped and the valve at the bottom of the tower is opened to remove old activated carbon in it, and flows to the bottom along with the water stage-by-stage and is released from the bottom of the tower.

1.8.2 Moving bed adsorption column

It is very effective when the length of adsorption bed is long. Waste water is supplied through a nozzle on the bottom of tower and discharged as treated water from a screen on the top (Figure 1.4).

1.8.3 Fixed bed adsorption column

Adsorption in fixed bed is an unsteady state process. In its analysis of basic importance are the space and the time distribution of the adsorbate (Figure 1.5). A graphical representation of the bed operation is a break through curve i.e. the dependence of adsorbate concentration in the effluent from the column on process duration. Break through time determines the period of protective action of the bed [14].

Conventional fixed bed processes involve a saturation, adsorption or loading step, followed by desorption, elution or regeneration steps. It comprise two drawbacks, one is the low efficiency of the fixed bed operation, since only a fraction of the adsorbent is used and the other is the use of a chemical regenerant to get an operative bed, with the associate waste disposal and a new pollution problem [21].

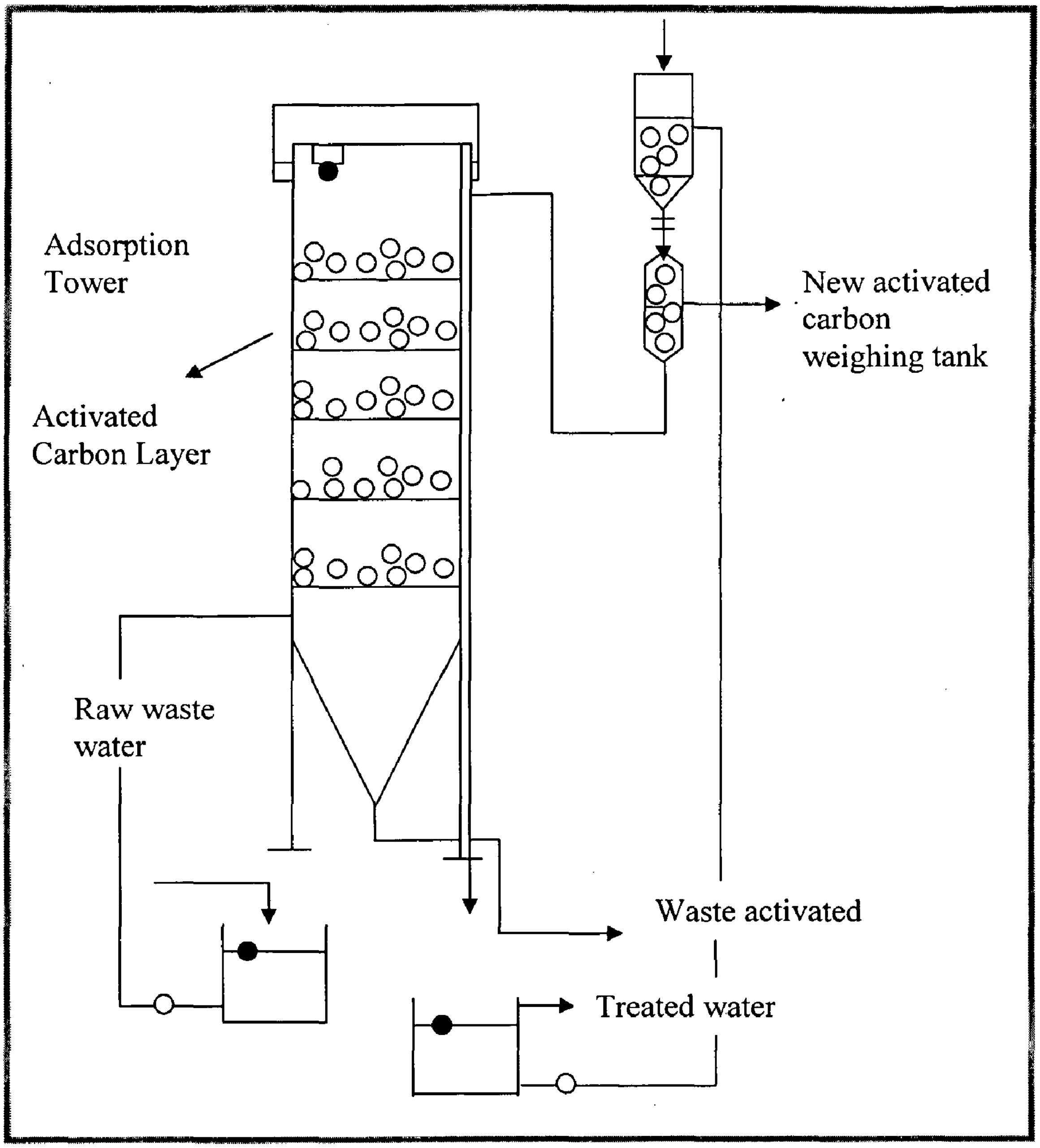

Figure 1.3: Fluidized bed adsorption column.

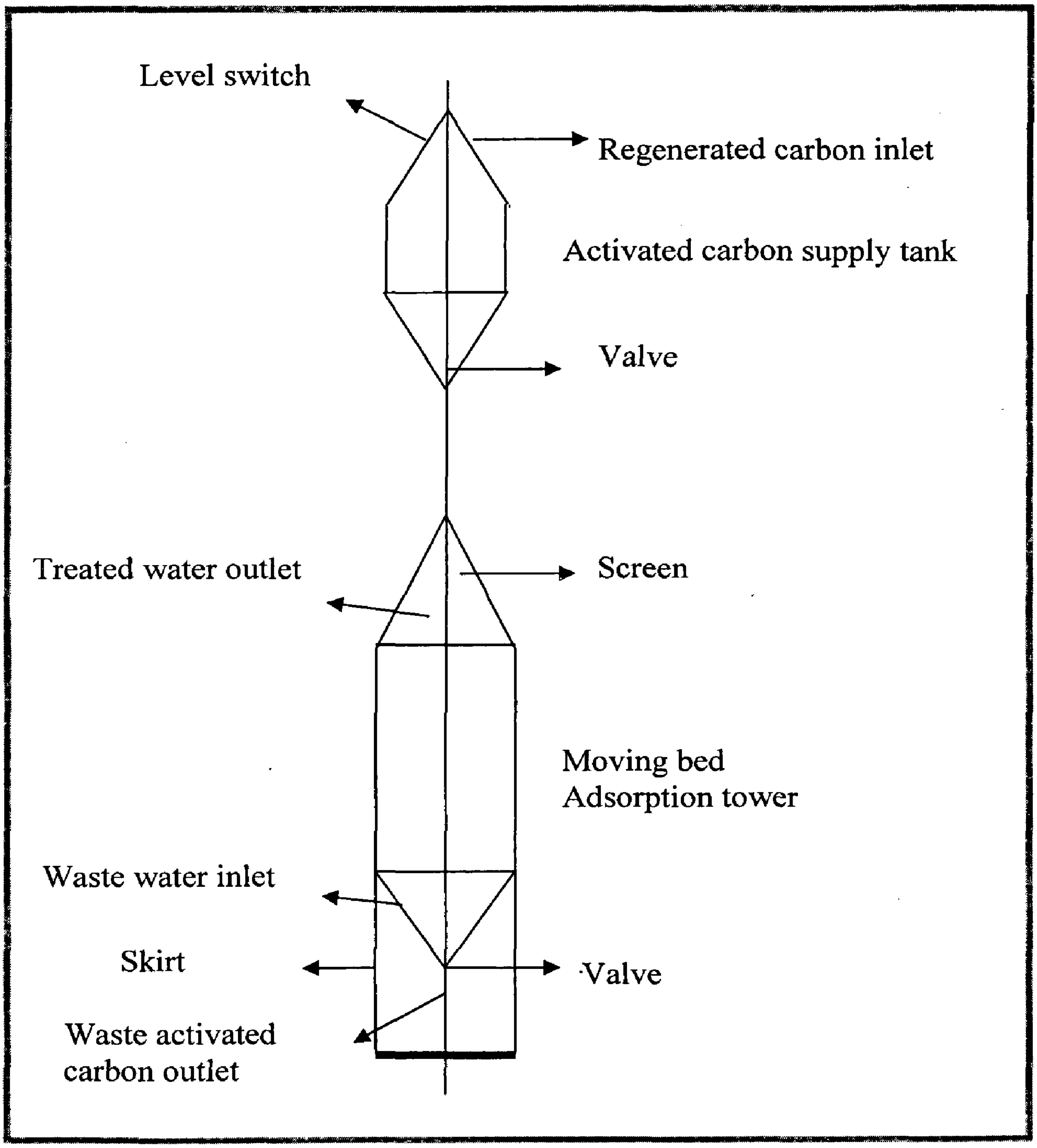

Figure 1.4: Moving bed adsorption tower.

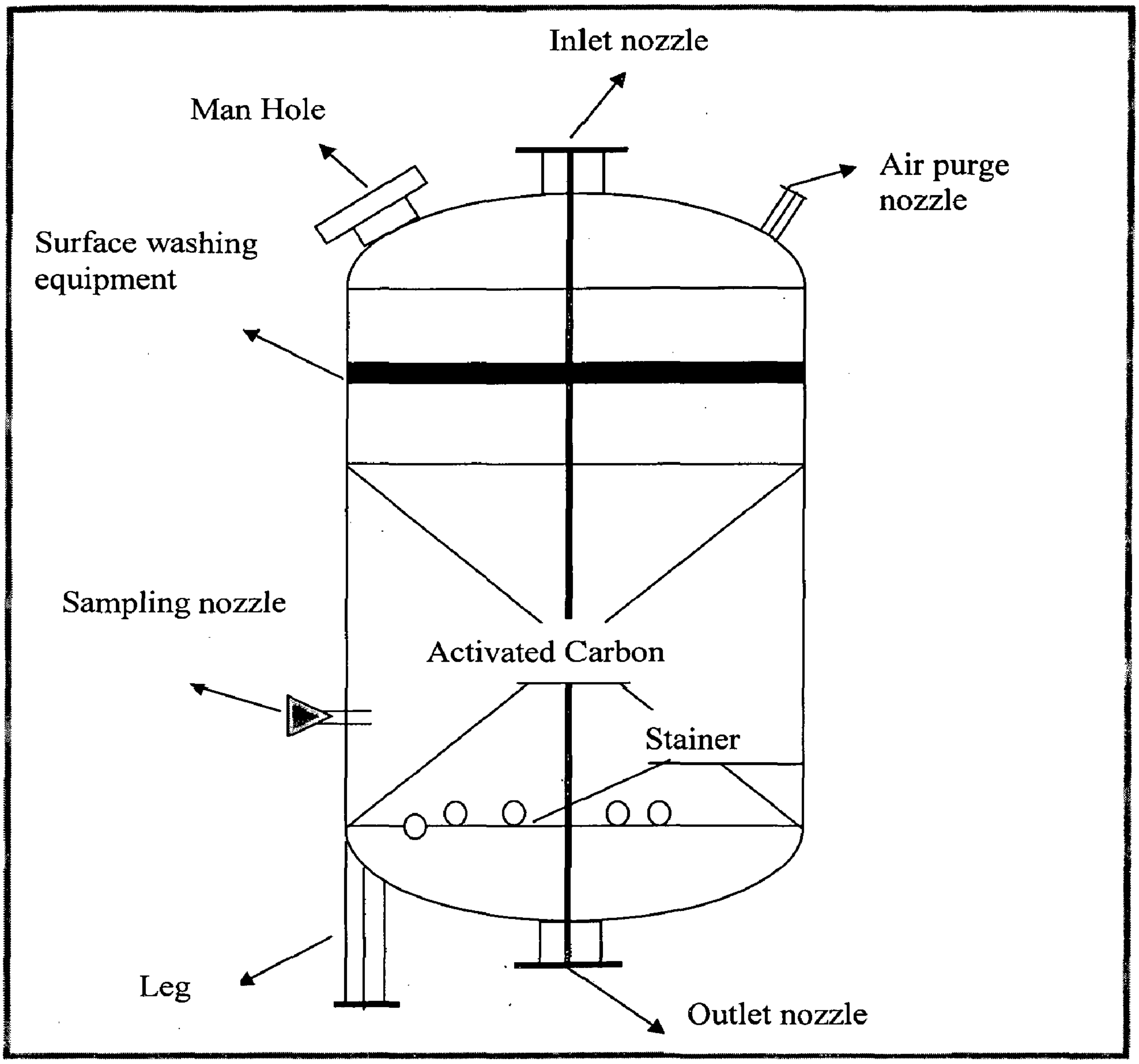

Figure 1.5: Fixed bed adsorption column.

1.8.3.1 Adsorption Uptake Rate

Important and integral to adsorption calculations and model formulations is the prediction or estimation of adsorbate uptake rates by adsorbent pellets. For the transport of adsorbates from the bulk of the fluid phase to the interior of a pellet before adsorption takes place, the following mass-transfer process may be present.

a) *Inter pellet mass transfer*: It refers to the diffusion and mixing of adsorbates in fluid occupying the spaces between the pellets. It is significant in fixed bed because adsorption treated solution is contacted with adsorbent pellets in relative motion.

b) *Inter phase mass transfer*: It refers to the transfer of adsorbate across the fluid pellet interface.

c) *Intra pellet mass transfer*: It refers to the diffusion of adsorbates within the pellet. It often takes place simultaneously with adsorption.

- **Inter pellet mass transfer**

In fixed bed adsorption, diffusion and mixing of adsorbates in fluid occurs as a result of adsorbate concentration gradients and non uniformity of fluid flow. This effect gives rise to dispersion of adsorbates, which takes place along both direction of main fluid flow (axial dispersion) and the direction transverse to the main flow direction(radial dispersion). Although the effect of axial dispersion is undesirable, since it reduces the separation efficiency, radial dispersion is usually considered helpful. Radial dispersion tends to equalize the differences in concentrations of small fluid elements at the same axial location; consequently, the undesired axial dispersion effect may be reduced. For liquids the axial peclet number approaches the theoretical value of 2.0 as the Reynolds number approaches 1000. For lower Reynolds number, peclet number is of the order 0.3 to 1.0. i.e, the dispersion effect is more significant.

- **Inter phase mass transfer**

It is an important step in the overall take up process. For single species adsorption with spherical particles, the inter phase mass transfer rate may be expressed as

$$\frac{d\bar{q}}{dt} = k_f a(C_b - C_s) = \frac{3k_f}{a_p \rho_p}(C_b - C_s) \tag{1.17}$$

The magnitude of k_f mass transfer coefficient depends on the flow conditions around the pellet and many empirical correlations are available in literature.

- **Intra pellet mass transfer**

The adsorbent materials are micro porous and their void is occupied by the fluid to be treated by adsorption, adsorbate may diffuse through pore fluid because of the presence of radial concentration gradient. This implies the existence of a similar concentration gradient in the adsorbed phase which, in turn causes the diffusion of the adsorbed molecules. Both types of diffusion may be operative simultaneously or individually. These two different mechanisms are pore and surface diffusion.

Pore diffusion: It is due to the diffusion of adsorbate molecules through the pore fluid. For the simple case of single species adsorption and assuming that Fick's law applies, the macroscopic conservation equation is given as

$$\varepsilon_p = \frac{\partial c}{\partial t} + \rho_p \frac{\partial q}{\partial t} = \frac{1}{r^2}\frac{\partial}{\partial r}\left[D_p r^2 \frac{\partial c}{\partial r}\right] \qquad 0 \le r \le a_p \tag{1.18}$$

where ' c ' and ' q ' are the adsorbate concentrations in the pore fluid and of the adsorbed phase corresponding to any given point within the pellet. Both pore diffusion and molecular diffusion involves the migration of adsorbate molecules in fluid phases. The semi empirical relation between pore diffusivity (D_{pe}) and molecular diffusivity (D_m) may be expressed as

$$D_{pe} = \frac{\varepsilon_p D_m}{\tau} \tag{1.19}$$

where τ is tortuosity factor of adsorbent which accounts for the fact that diffusion takes place zigzag wise rather than along the radial direction.

In the limiting case in which the pores are small (to the extent that pore radius is less than the mean free path of the fluid molecules), collisions of fluid molecules with the pore surface dominate resulting in an entirely different type of diffusion, known as Knudsen diffusion. In the pore both molecular and Knudsen diffusivity, D_K may be operative simultaneously, D_p should be replaced by $\overline{D}_p$ which is defined as

$$\frac{1}{\overline{D}_p} = \frac{1}{D_p} + \frac{1}{D_K} \tag{1.20}$$

Surface diffusion: It is the case in which the intra pellet mass transfer is affected through the diffusion of adsorbed molecules, for single species adsorption with spherical pellets and assuming that Fick's law applies, and is described by the following equation.

$$\left(\frac{\varepsilon_p}{\rho_p}\right)\frac{\partial c}{\partial t}+\frac{\partial q}{\partial t}=\frac{1}{r^2}\frac{\partial}{\partial r}\left[D_s r^2\frac{\partial q}{\partial r}\right] \tag{1.21}$$

here the term $\left(\frac{\varepsilon_p}{\rho_p}\right)\left(\frac{\partial c}{\partial t}\right)$ is much less than $\partial q/\partial t$ so it can be easily solved with appropriate initial and boundary conditions. The parameter D_s vary with both temperature and extent of surface coverage (q). For the liquid systems it is found to be in the range of 10^{-9} to 10^{-7}cm^{2}s^{-1}.

Combined pore and surface diffusion: For more general description of intra pellet mass transfer, it is appropriate to assume that both pore and surface diffusion are operative. The corresponding macroscopic conservation equation for a spherical pellet becomes

$$\varepsilon_p\frac{\partial c}{\partial t}+\rho_p\frac{\partial q}{\partial t}=\frac{1}{r^2}\frac{\partial}{\partial r}\left[D_p r^2\frac{\partial c}{\partial r}\right]+\frac{\rho_p}{r^2}\frac{\partial}{\partial r}\left[D_s r^2\frac{\partial q}{\partial r}\right] \tag{1.22}$$

For physical adsorption, since the actual adsorption step occurs much faster than does mass transfer step, the pore solution concentration and the adsorption concentration may be assumed equilibrium i.e q = f(c) is the isotherm expression. And dq = f'(c) dc. Substituting and rearranging one has

$$\varepsilon_p\frac{\partial c}{\partial t}+\rho_p\frac{\partial q}{\partial t}=\frac{\rho_p}{r^2}\frac{\partial}{\partial r}\left[D_e r^2\frac{\partial q}{\partial r}\right] \tag{1.23}$$

where effective intra particle diffusivity D_e is defined as

$$D_e=\frac{D_p}{f'(c)}\frac{1}{\rho_p}+D_s \tag{1.24}$$

In the limiting case either pore diffusion or surface diffusion dominates.

- **Intra pellet mass transfer**

It refers to the diffusion of adsorbates within the pellet. It often takes place simultaneously with adsorption.

In physical adsorption of adsorbate from the solution phase onto adsorption site occurs due to the difference between the adsorbates chemical potential in the solution and adsorbed phases. In most cases, it occurs much faster than various transport steps and can therefore be ignored when formulating the overall rate expression [24].

1.8.3.2 Intra Pellet Diffusion-Linear Driving Force Model

Regardless of the diffusion mechanism is used to describe the transport of adsorbate, a quantitative representation of adsorbate uptake rate requires the solution of the appropriate intra particle diffusion equation. To simplify calculations, the so-called lumped parameter model has been developed. In essence, t is postulated that the uptake rate of adsorbate by pellet is linearly proportional to a driving force, defined as the difference between the surface concentration and the average adsorbed-phase concentration can be written as

$$\frac{d\bar{q}}{dt} = k_p\left(q_s - \bar{q}\right) \tag{1.25}$$

where k_p is particle phase transfer coefficient, $\bar{q}$ and q_s are the average adsorbed phase concentration and the adsorbed phase concentration at the exterior surface of the pellet.

$$k_p = \frac{15D_e}{a_p^2} \tag{1.26}$$

D_e is effective particle diffusivity when both surface and pore diffusivity's are present. In the limiting cases that either pore or surface diffusion is the controlling mechanism we will have

$$k_p = \frac{15D_s}{a_p^2} \quad \text{(Surface diffusion)} \tag{1.27}$$

$$k_p = \frac{15D_p}{a_p^2 f'(c)\rho_p} \quad \text{(Pore diffusion)} \tag{1.28}$$

1.8.3.3 Break through Curve

Adsorption is unsteady state process. A graphical representation of the bed operation is a break through curve is dependence of adsorbate concentration in the effluent from the column on process duration. Break through time determines the period of protective action of the bed [14]. To remove the phenol, the waste water flows through adsorption bed. Figure 1.6 shows the idealized breakthrough curve as a function of the liquid volume to be treated.

After short working time the adsorbent bed is subdivided into three zones:

- On the inlet side of the adsorber the equilibrium load corresponding to the inlet concentration c_0 is achieved.
- Next follows the adsorbate reduction in the so called adsorption or mass transfer zone (MTZ).
- The outlet zone of the adsorber filling is still unloaded at this time.

With increasing adsorption time the adsorption zone moves through the bed. If the top of the MTZ reaches the adsorber end breakthrough occurs. The adsorption step will be stopped if a pre-determined solvent concentration in the exhaust liquid is exceeded. Then the bed has to be regenerated. If the passage of the fluid is continued on still further, the exit concentration continues to rise until it becomes the same as the inlet concentration.

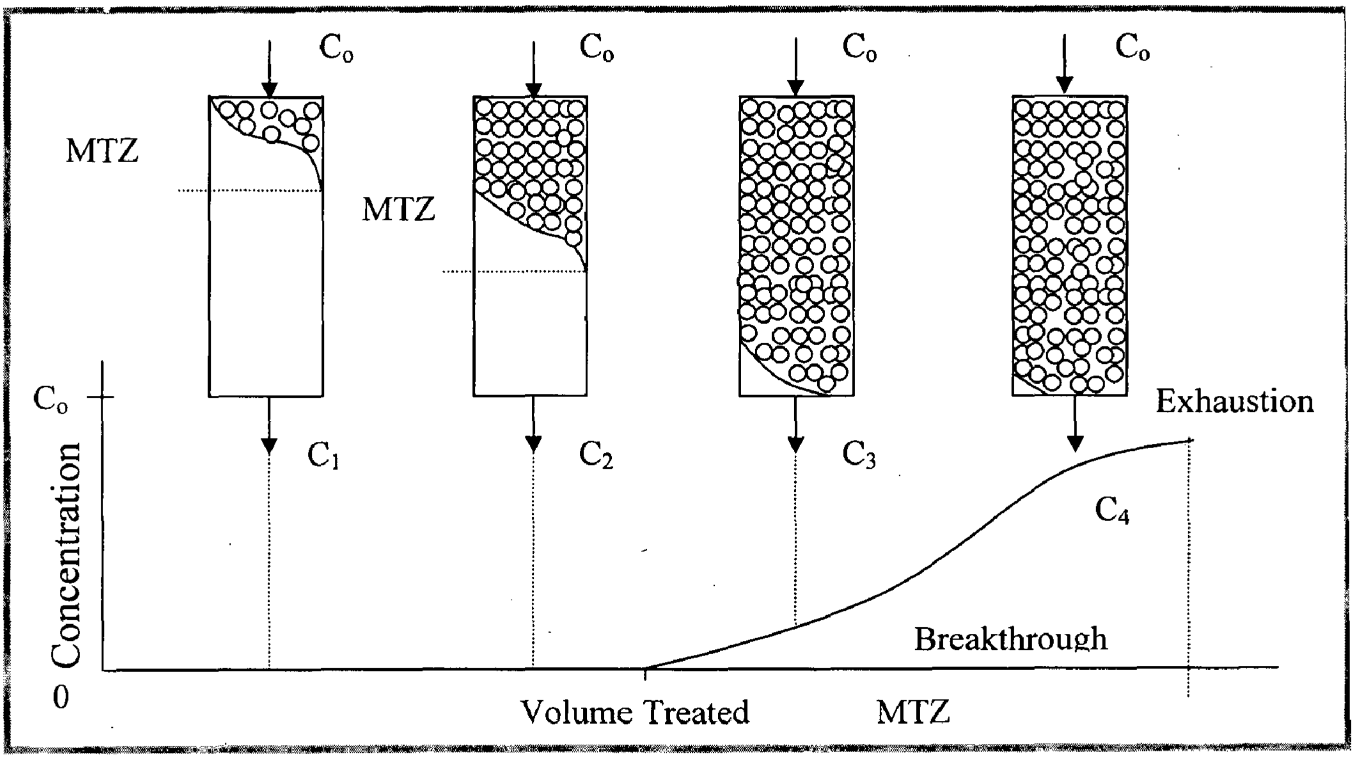

Figure 1.6: Idealized breakthrough curve of a fixed bed adsorber.

The shape and time of appearance of break through curve greatly influence the method of operating a fixed bed adsorber. The curves generally have an S-shape, but they may be steep or relatively flat and in some cases considerably distorted. If the adsorption process were infinitely rapid, the break through curve would be a straight vertical line in the lower part of figure 1.6. The actual rate and mechanism of adsorption process, the nature of adsorption equilibrium, the fluid velocity, the concentration of solute in the feed, and the length of the adsorber bed (particularly if the solute concentration in the feed is high) all contribute to the shape of the curve produced for any system. The break point is very sharply defined in some cases and in other cases poorly defined.

Generally the break time decreases with decreased bed height, increased particle size of adsorbent, increased rate of flow of fluid through the bed, and increased initial solute content of the feed. There is a critical minimum bed height below which the solute concentration in the effluent rise rapidly from the first appearance of effluent. In planning new processes it is best to determine the break point and break through curve for a particular system experimentally under conditions resembling as much as possible those expected in the process.

1.9 DESCRIPTION OF THE PROBLEM

Aromatic compounds such as phenols occur in waste water of a number of industries such as high temperature coal conversion, petroleum refining, resin, pharmaceutical, plastic, and pesticidal chemical industries. Such aromatic hydroxy compounds can be toxic when present in elevated levels and are known or suspected to be carcinogens. However, phenol is toxic to aquatic life and humans even at low concentrations (5-25 mg L^{-1}). Phenol is listed as a priority pollutant by the United States Environmental Protection Agency (EPA) and results in oxygen demand in receiving waters and objectionable tastes to drinking water. Chronic toxic effects due to these reported in humans include vomiting, difficulty in swallowing, anorexia, liver and kidney damage, headache, fainting and other mental disturbances. Thus, the removal of such chemicals from industrial effluents is of great importance. The MOEF has set a maximum concentration level of 1.0 mg/l of phenol in the industrial effluents for safe discharge into surface waters, WHO recommends the permissible phenolic concentration of 0.001 mg/l in potable waters [26].

Current methods for removing phenolics from wastewater include microbial degradation, adsorption on activated carbon, chemical oxidation (using agents such as ozone, hydrogen peroxide or chlorine dioxide), incineration methods, solvent extraction and irradiation. The choice of system depends on economic and other factors [28]. Biodegradation of phenol occurs very slowly or does not occur at all lead to setting up of rigid limits on the acceptable level of phenol in the environment. Adsorptive processes are widely used as secondary or polishing treatment in purification of such polluted streams and diluted waste waters.

Phenol, a derivative of benzene, is an important raw material in petrochemicals, oil refineries, leather, paint, steel industries, pharmaceuticals, plastic and pesticide industry [26]. Phenol is usually used to synthesize chemical products in basic solution .because of its low solubility in acidic and neutral solution. Therefore, the effluents from these chemical plants containing phenol are basic.

CHAPTER 2

LITERATURE REVIEW

2.1 EXPERIMENTAL STUDIES

Rengaraj et al. (2002) studied that, how the activated carbon prepared from rubber seed coat (RSCC), an agricultural waste by-product, has been used for the adsorption of phenol from aqueous solution. In this work, adsorption of phenol on rubber seed coat activated carbon has been studied by using batch and column studies. The equilibrium adsorption level was determined to be a function of the solution pH, adsorbent dosage and contact time. The equilibrium adsorption capacity of rubber seed coat activated carbon for phenol removal was obtained by using linear Freundlich isotherm.

The adsorption of phenol on rubber seed coat activated carbon follows first order reversible kinetics. The suitability of RSCC for treating phenol based resin manufacturing industry wastewater was also tested. A comparative study with a commercial activated carbon (CAC) showed that RSCC is 2.25 times more efficient compared to CAC based on column adsorption study for phenolic wastewater treatment.

Qadeer and Rehan (2002) studied that commercial active carbon was tested as an adsorbent for the removal of phenol from aqueous solutions. The optimum conditions for maximum adsorption in terms of shaking time, amount of the adsorbent, and concentration of the adsorbate were identified. The adsorption data fitted the Langmuir isotherm equation in the whole range of concentrations studied. The adsorption of picric acid, pyrogallol and salicylic acid at selected conditions for phenol was also studied. Elution studies to recover the adsorbed phenol from active carbon were performed with distilled water, NaOH and HCl solutions.

It is concluded that active carbon can be used to remove phenol from aqueous waste solutions before discharging into the hydrosphere. The method is simple, economical, fast and requires no chemical treatment. Adsorbed phenol can be eluted and used as a raw material in different industries while active carbon column could be reused, thus no waste management problem arises.

Kumar et al. (2003) they carried out investigations in the batch mode for studying the adsorption behavior of resorcinol and catechol on granular activated carbon from a basic salt medium (BSM) at pH≈7.1 and temperature≈30 8C. The isotherm data were correlated with six isotherm models, namely Langmuir, Freundlich, Redlich-Peterson, Radke-Prausnitz, Toth, and Fritz–Schlunder's using a nonlinear regression technique. It is observed that the catechol isotherm data may be represented by Redlich-Peterson, Radke–Prausnitz, Toth, and Fritz–Schlunder models with similar accuracy (max. dev. 12%). And the resorcinol data may be represented by Freundlich, Redlich-Peterson, Radke–Prausnitz, and Fritz–Schlunder models equally well (max. dev. 15%). Freundlich being a simple model is recommended for resorcinol.

At the conditions investigated in this study, catechol is adsorbed to a greater extent than resorcinol. This is due to the compound's solubility and position of the –OH group on the benzene aromatic ring. The kinetics of adsorption have been found to be diffusion controlled and the value of effective particle diffusion coefficients is of the order of $10^{-13} m^2/s$. Three distinct phases of kinetics-rapid, medium, and slow-have been observed. These results should be useful for the design of adsorbers for removing these pollutants.

Kujawski et al. (2003) studied that the application of membrane techniques (pervaporation and membrane-based solvent extraction) and adsorption to the removal of phenol from solutions modeling wastewater from phenol production by cumene oxidation process was investigated. The transport and separation properties of composite membranes PEBA, PERVA 1060 and PERVAP 1070 in pervaporation of water-phenol mixtures were determined. It was found that the best removal efficiency of phenol was obtained using the PEBA membrane. MTBE, cumene and the mixture of hydrocarbons were applied. Extra-Flow contactor with Celgard X-30 polypropylene hollow fibre porous membrane was used in the experiments. MTBE was found the most efficient extraction. Adsorption of phenol on the different Amberlite resins was also investigated. Among the Amberlite resins of various grades used, the Amberlite XAD-4 had the best properties in the phenol removal from the aqueous solution. It was shown that regeneration of the adsorbent bed could be effectively performed with sodium hydroxide solution.

Akarsu et al. (2003) studied that adsorbent powders were prepared from the uncatalysed hydrolysis-condensation reactions of different complexes that were synthesized by the reactions of $Zr(OPr^n)_4$ with different chelating ligands (such as allyl acetic acid [AAH], vinyl acetic acid [VAH] and citraconic acid [CAH]). The complex products were characterized by FT-IR, ^{1}H-NMR and ^{13}C-NMR spectra. The maximum combination ratios of $AAH/Zr(OPr^n)_4$, $VAH/Zr(OPr^n)_4$ and $CAH/Zr(OPr^n)_4$ were 1.7, 0.9 and 1.3, respectively. The hydrolysis-condensation products of these complexes were calcinated at 900^0C and half of them were coated with 3-glycidyloxypropyltrimethoxysilane (GLYMO). The surface area and average pore diameter of the powders were estimated by the analysis of adsorption/desorption BET isotherm data. The adsorption capacities of these powders for aqueous phenol and p-chlorophenol were calculated following spectrophotometric determination. Phenol and p-chlorophenol adsorption on all of the GLYMO-coated adsorbents were satisfactory, e.g., the adsorbent obtained from the hydrolyzed, calcinated and GLYMO coated form of $Zr(OPr^n)_{2:3}(AA)_{1:7}$ adsorbed 63% of phenol while the uncoated form adsorbed only 10%. The adsorption isotherm has been determined and data have been analyzed according to the Freundlich model.

He concludes that new metal-organic adsorbent powders were prepared and tested for phenol and p-chlorophenol, which are known contaminants in many industrial wastewaters. The adsorptive capacity of the adsorbent was limited (0.11-1.20 mg/g). Adsorption was strongly dependent on the initial concentrations of the solutions. The capacity increased with the increase in the initial concentrations of phenol and p-chlorophenol. The Freundlich constant, 'a' was 1.15 and 1.33 for phenol and p-chlorophenol, respectively. We observed that 'a' is almost equal to unity. Therefore, the adsorption of phenol is more favorable than p-chlorophenol adsorption.

Ghiasi et al. (2004) studied nonionic organic contaminants (NOCs) such as benzene, toluene, and phenol from contaminated wastewater can be effectively adsorbed by organo-zeolites. Organo-zeolites were prepared from synthetic ZSM-5 and natural zeolites, by exchanging quaternary amines, i.e. hexadecyltrimethyl ammonium (HDTMA) bromide and *n*-cetylpyridinium bromide (CPB). The maximum adsorption of CPB onto these zeolites is in the order of clinoptilolite > ZSM-5-88 (SiO_2/Al_2O_3 = 88) > ZSM-5-31 (SiO_2/Al_2O_3 = 31) which is mainly dependent on the external cation exchange capacity (ECEC) of each zeolite. Batch adsorption experiment was carried out to remove benzene, toluene, and phenol from aqueous solution using the above-mentioned organo-zeolites. In addition, as-synthesized MCM-41 molecular sieve was employed for removal of organic contaminants from aqueous solution. The experimental results were fitted to the Langmuir, Freundlich, Redlich–Peterson and linear equation isotherms to obtain the characteristic parameters of each model. Our resultant data showed that nonlinear form of Langmuir, the Freundlich and Redlich–Peterson could be fitted well with sorption data in most cases. According to the evaluation using the Langmuir equation, the maximum organics adsorption by synthesized MCM-41 was much greater than that of the natural clinoptilolite and ZSM-5 zeolites.

The adsorption of benzene, toluene and phenol by CPB and HDTMA surfactants modified ZSM-5-31, ZSM-5-88, and clinoptilolite besides as-synthesized MCM-41 molecular sieve were investigated. The increase in NOCs (benzene, toluene and phenol) concentration or initial concentrations of surfactants resulted in an increase in the NOC adsorption by the sorbents tested in this work.

Ozkaya (2006) studied the adsorption of phenol from aqueous solutions presents the most widespread uses of activated carbons in water treatment. The three-parameter isotherm models as well as two-parameter models were found to be applicable for the adsorption equilibrium data by non-linear regression. The low value of desorption kinetic constant indicates that the adsorbed phenol remains almost stable on the adsorbent and can be recovered from the adsorbent by desorption with sodium hydroxide. The results showed that the first-order kinetic model represented the data for NaOH desorption more suitable fitting than the pore diffusion model. The results also demonstrated that the Langmuir model fitted the experimental data a little better than the three parameter models, Redlich–Peterson and Toth. It is determined that the standard errors were minimum level in fitted three models.

Nagda et al. (2007) studied that the potential of tendu (Diospyros melanoxylon) leaf refuse from bidi industry waste to remove phenol from aqueous solution was studied. For this purpose, the tendu leaf refuse was carbonized by subjecting it to chemical treatments with sulfuric acid. Batch kinetics and isotherm studies were carried out under varying experimental conditions of contact time, phenol concentration, adsorbent dose and pH. Adsorption equilibrium of tendu leaf refuse and chemically carbonized tendu leaf refuse was reached within 2 hr for phenol concentration 10-25 mg/l and 1 hr for phenol concentration 20-200 mg/l, respectively. The adsorption of phenol decreases by the increase of the pH value of the solution. The kinetic data followed more closely the pseudo-second-order chemisorption model. The adsorption data were modeled by using both Langmuir and Freundlich classical adsorption isotherms. The maximum adsorption capacity of chemically carbonized tendu leaf refuse as per Langmuir model was 4 times higher than that of raw tendu leaf refuse. The results illustrate how tendu leaf refuse, a solid waste disposal menace from bidi industry, can be used as an effective biosorbent for phenol in aqueous solution.

Mukherjee et al. (2007) studied that the adsorption process is gaining interest as one of the effective processes of advanced wastewater treatment for treatment of industrial effluent containing toxic materials. The present work involves an investigation of the use of three carbonaceous materials, activated carbon (AC), bagasse ash (BA) and wood charcoal (WC), as adsorbents for removal of phenol from water. Batch experiments were carried out to obtain adsorption equilibrium isotherms and kinetics with phenol spiked synthetic solutions. The study was performed with two initial phenol concentrations, viz. 30 and 50 mg/L, with an equal amount of adsorbent dose (50 g/L). The effects of solution pH, concentrations of EDTA, anions, and dosages of adsorbent on removal of phenol were examined. Desorption tests were also conducted in the present study. The suitability of the different isotherm models to the equilibrium data was studied for each phenol–adsorbent system. Experimental results showed that for phenol–AC, phenol–WC and phenol–BA adsorption systems, approximately 98%, 90% and 90% removal efficiencies were achieved at given adsorption conditions. The kinetic study indicates that the phenol removal with the selected adsorbents is a first order adsorption. Freundlich isotherm model was found to fit the data for adsorption of phenol with the adsorbents. Removal efficiency of phenol slightly increased when the pH of adsorption system decreased. The effect of nitrate ion and EDTA in the solution on the adsorption of phenol was found to be insignificant; however, the chloride ion has considerable negative effects on the removal by BA. The estimation of diffusion coefficients indicated that film diffusion may control the adsorption of phenol with the studied adsorbent materials.

Hameed and Rahman (2008) studied that activated carbon derived from rattan sawdust (ACR) was evaluated for its ability to remove phenol from an aqueous solution in a batch process. Equilibrium studies were conducted in the range of 25–200 mg/L initial phenol concentrations, 3–10 solution pH and at temperature of 30 °C. The experimental data were analyzed by the Langmuir, Freundlich, Temkin and Dubinin–Radushkevich isotherm models. Equilibrium data fitted well to the Langmuir model with a maximum adsorption capacity of 149.25 mg/g. The dimensionless separation factor R_L revealed the favorable nature of the isotherm of the phenol-activated carbon system. The pseudo-second-order kinetic model best described the adsorption process. The results proved that the prepared activated carbon was an effective adsorbent for removal of phenol from aqueous solution.

The activated carbon prepared from biomass can be effectively used as adsorbent for the removal of phenol from aqueous solutions. The solution pH played a significant role in influencing the capacity of an adsorbent towards phenol molecules. A decrease in the pH of solutions led to a significant increase in the adsorption capacity of activated carbon. The obtained results showed that the ACR possessed a high adsorption capacity to remove phenol. The Langmuir, Freundlich, Temkin and Dubinin–Radushkevich isotherm models were used to express the sorption phenomena of phenol to the prepared activated carbon. Consequently, linear regression of the experimental data showed that the Langmuir equation best represented phenol adsorption data. The maximum adsorption capacity of ACR was 149.25 mg/g. The pseudo-first order and pseudo-second-order kinetic models were used to analyze the data obtained for phenol adsorption onto the prepared activated carbon. The results indicated that the pseudo-second order equation provided the better correlation for the adsorption data.

Stavropoulos et al. (2008) studied that the activated carbons with various surface functional groups and tailored adsorption capacity were produced by the application of different oxidation techniques. Samples treated by urea presented basic characteristics, which enhanced the removal capacity of phenols; the enhancement of the phenol adsorption was associated to the increased nitrogen content of these samples. Activated carbons treated by oxygen and nitric acid presented significant acidic character and a lower phenol adsorption capacity. Furthermore, the oxidation treatment affected the pore structure development in different modes: oxygen gasification slightly affected the surface area and pore volumes of the produced samples, while the highest reduction in pore structure was observed for the samples treated by nitric acid solutions. As a result, urea and possibly other nitrogenous compounds may be used as effective mediums for the enhancement of phenol adsorption potential in activated carbons.

2.2 MODELING STUDIES

Costa et al. (1982) studied a new process for purification of phenolic waste water by parametric pumping is presented. An equilibrium (linear) model for non-mixed dead volumes thermal direst mode parametric pumping is developed and the influence of bottom and top dead volume magnitudes on transient separation is analyzed. It tells us that for each bottom dead volume magnitude there is a minimum top dead volume that should be maintained in order to get an improved transient separation, relatively to the mixed case where inexistence of the top dead volume gives a better separation. Analytical solutions for batch, continuous and semicontinous operations are presented. Experimental studies on the system phenol/water-Duolite ES861 include equilibrium isotherms at 20°C and 60°C and par pump runs for the cases mentioned above.

Otero et al. (2005) he studied that phenol is a target pollutant to be removed from wastewaters from different industries. Adsorption of phenol from aqueous solutions onto two polymeric resins (Sephabeads SP206 and SP207) and onto activated carbon (Filtrasorb F400) was studied. Batch equilibrium experiments were carried out at three different temperatures (293, 310 and 333 K) for each of the adsorbents. In order to ascertain the fixed bed performance of the adsorbents considered adsorption runs were carried out at laboratory scale at 293, 310 and 333 K. Equilibrium and fixed bed experimental results were compared to the simulated ones. Equilibrium data were well fitted by the Langmuir isotherm and the breakthrough curves simulation was based on this equilibrium isotherm together with a mass transfer description based on the Linear Driving Force (LDF) model. After the adsorbents screening and mass transfer parameters determination, Sephabeads SP206 was used to purify a phenolic solution by parametric pumping at pilot scale using hot and cold temperatures of 293 and 333 K respectively. The adsorbent Sephabeads SP206 is the one which adsorption performance is affected by temperature in a higher degree. A package for the simulation of this cyclic operation was used to predict model results, which were satisfactorily compared to those experimentally obtained.

The mass balance in a bed volume element is

$$D_{ax}\frac{\partial^2 C(z,t)}{\partial z^2}-u_i\frac{\partial C(z,t)}{\partial z}=\frac{\partial C(z,t)}{\partial t}+\frac{(1-\varepsilon)}{\varepsilon}\rho_p f_h\frac{\partial q<(z,t)>}{\partial t}$$

The boundary conditions are Danckwerts boundary condition

$$z=0,\quad t\geq 0 \qquad D_{ax}\left.\frac{\partial C(z,t)}{\partial z}\right|_{z=0}=u_i\left(C(0,t)-C_0\right)$$

$$z=L,\quad t\geq 0 \qquad \left.\frac{\partial C(z,t)}{\partial z}\right|_{z=L}=0$$

where

D_{ax}	Axial dispersion, m^2/s
C	Concentration in the bulk fluid phase, mg/l
z	Axial coordinate in the bed, m
t	Time, s
u_i	Interstitial velocity, m/s
ε	Bed porosity
ρ_p	Density of the adsorbent, kg/m^3
f_h	Humidity factor
q	Solute adsorbed per dry mass of adsorbent at a certain time, mg/g
C_0	Initial liquid-phase concentration of phenol, mg/l

Pan et al. (2005) he studied that removal of many organic pollutants including phenolic compounds from industrial wastewater can always be achieved by fixed-bed adsorption onto the polymeric resin adsorbent, and the relevant breakthrough curves would provide much valuable information to help to design a fixed-bed adsorption process in field application. In the present study, The adsorption rate can be described by the linear driving force model in terms of the overall liquid-phase mass-transfer coefficient, a model developed based on the constant-pattern wave approach theory and the Freundlich model was adopted to describe the breakthrough curves of phenol and p-nitrophenol adsorption onto a macro reticular resin adsorbent NDA100 from aqueous solution.

Column experiments were performed at different conditions to verify the model and the results proved that the model would describe the breakthrough curves well. Effect of the operation parameters on breakthrough curves was also discussed to get helpful information in choosing the adsorption process. $t_{1/2}$ decreases and $K_L a$ increase with increasing feed flow rate, which is consistent with conclusion that $K_L a$ varied linearly with the feed flow rate.

The $t_{1/2}$ values decrease with increasing C_F, on the other hand, $K_L a$ increases slightly with increasing C_F. This means the breakthrough curve is steeper at higher CF. $t_{1/2}$ value is roughly proportional to the bed height at a given U_0. On the other hand; increasing bed height has little effect on the $K_L a$. The values of $t_{1/2}$ and $K_L a$ decrease with increasing temperature because the adsorption of phenols onto resin NDA-100 can be considered as physical adsorption, Different aspect ratios at given amount of resin adsorbent have little effect on the breakthrough curves, a too large value of aspect ratio is not essential when designing adsorption process in field application.

The governing equation for predicting column dynamics is

$$\varepsilon \frac{\partial C}{\partial t} + u_o \varepsilon \frac{\partial C}{\partial z} + \rho \frac{\partial q}{\partial t} = 0$$

This equation is unsteady state mass balance for adsorbate. The adsorption rate can be described by the linear driving force model in terms of the overall liquid-phase mass-transfer coefficient.

$$\rho \frac{\partial q}{\partial t} = \varepsilon K_L a \left(C - C^* \right)$$

$$C^* = f(q)$$

The breakthrough curve can be calculated by the following equation

$$t = t_{1/2} + \frac{\rho q_F}{\varepsilon K_L a C_F} \int_{C_F/2}^{C} \frac{1}{C - g\left(q_F \, C/C_F \right)} dC$$

where

ρ Resin bed density, g/L

ε Void fraction of bed

C Phenol concentration in mobile phase, $mmol/L$

t	Time, h
u_o	Interstitial fluid velocity, cm/h
z	The distance from the inlet of mobile phase, m
q	Phenol concentration in stationary phase, $mmol/g$
$K_L a$	Volumetric coefficients in liquid-phase, h^{-1}
$t_{1/2}$	Half time, h
q_F	Phenol concentration in stationary phase, $mmol/g$
C_F	Feed phenol concentration in mobile phase, $mmol/L$

Aribike and Olafadehan (2008) did Mathematical modeling of liquid phase adsorption of phenols in fixed beds of granular activated carbon was investigated. The model considered the effects of axial diffusion in the fluid, the external film and internal diffusional mass transfer resistances of the particles, and the nonlinear adsorption isotherm of Freundlich.

It was shown that the analysis of a complex multicomponent adsorption system could be simplified by converting it into a pseudo single-component adsorption system. This was achieved by lumping the concentrations of the components together as one single parameter, chemical oxygen demand. The resulting model equations were solved using the orthogonal collocation method and third-order semi-implicit Runge-Kutta method combined with a step-size adjustment strategy. Excellent agreement between simulated results and pilot plant data was obtained. Also, the breakthrough profiles revealed the formation of a primary monomolecular layer on the adsorbent surface.

The differential mass balance for the adsorbate in the pore fluid is given by

$$\frac{\varepsilon_p}{r^2}\frac{\partial}{\partial r}\left(r^2 D_{pi}\frac{\partial X_i}{\partial r}\right)=\varepsilon_p\frac{\partial X_i}{\partial t}+\sum_{i=1}^{n}\left(\frac{\partial q_i^*}{\partial X_i}\right)\left(\frac{\partial X_i}{\partial t}\right)$$

subject to the initial and boundary conditions:

$$X_i = 0 \qquad (t=0, 0<r<R, 0\le z\le z_T)$$

$$\varepsilon_P D_{Pi}\left(\frac{\partial X_i}{\partial r}\right)\bigg|_{r=R} = K_{fi}(C_i - X_i) \qquad (0\le z\le z_T, 0<r<R, t>0)$$

$$\left(\frac{\partial X_i}{\partial r}\right)\Bigg|_{r=R} = 0 \qquad \left(0 \le z \le z_T, 0 < r < R, t > 0\right)$$

A differential material balance applied to the adsorbate carried by the following fluid stream gives the following:

$$\frac{\partial C_i}{\partial t} = D_{L1}\frac{\partial^2 C_i}{\partial z^2} - U_f\frac{\partial C_i}{\partial z} - \left(\frac{1-\varepsilon_b}{\varepsilon_b}\right)\left(\frac{3}{R}\right)K_{fi}\left(C_i - X_i\right)$$

The initial and boundary conditions required are

$$C_i = C_{oi} \qquad \left(t = 0, 0 \le z \le z_T\right)$$

$$U_f C_{oi}(t) - U_f C_i\Big|_{Z=0} + D_{L1}\left(\frac{\partial C_i}{\partial z}\right)\Bigg|_{Z=0} = 0 \qquad (t > 0)$$

$$\left(\frac{\partial C_i}{\partial z}\right)\Bigg|_{Z=Z_T} = 0 \qquad (t > 0)$$

By orthogonal collocation method, above set of non linear PDEs are converted to Boundary value problem of ODEs.

$$\frac{d\overline{C}_{1,j}}{d\tau} = \sum_{k=1}^{N+1} T_{j,k}\overline{C}_{1,k} - \psi_3\sum_{k=1}^{NR} A'_{N+1,k}\overline{X}_{1,k} + \psi_1\overline{C}_{1,j} + \overline{Pe}_1$$

where

$$T_{j,k} = \psi_2\left(B_{j,N+2}A''_{1,k} + B_{j,1}A'_{1,k} + B_{j,k}\right) - \psi_1\left(A_{j,N+2}A''_{1,k} + A_{j,1}A'_{1,k} + A_{j,k}\right)$$

$$\overline{\psi}_1 = \psi_3\left(\Phi_1 - 1\right)$$

$$\overline{Pe}_1 = \psi_2\left(B_{j,N+2}Pe''_1 + B_{j,1}Pe'_1\right) - \psi_1\left(A_{j,N+2}Pe''_1 + A_{j,1}Pe'_1\right)$$

and

$$\frac{d\overline{X}_{1,j}}{d\tau} = \frac{\varepsilon_p A}{\alpha_1 R^2}\left(\sum_{k=1}^{NR}\overline{U}_{j,k}\overline{X}_{1,k} + \psi_4\overline{C}_{1,j}\right)$$

where

$$\overline{U}_{j,k} = 4\sigma_j\left(B_{j,k} - B_{j,N+1}A'_{N+1,k}\right) + 6\left(A_{j,k} - A_{j,N+1}A'_{N+1,k}\right)$$

$$\psi_4 = \Phi_1\left(4\sigma_j B_{j,N+1} + 6A_{j,N+1}\right)$$

where

$A_{j,k}$	constant generated in the orthogonal collocation method
$B_{j,k}$	constant generated in the orthogonal collocation method
Ci	concentration of solute *i* in fluid phase of the column, kg/m^3
C_{oi}	inlet concentration of solute *i* in the column, kg/m^3
D_{L1}	axial diffusivity for component *i* in the fluid phase, m^2/s
D_{pi}	diffusivity for component *i* in the fluid phase within the pore, m^2/s
q_i^*	concentration of solute *i* in the solid phase, kg/m^3
q_{oi}^*	concentration of adsorbed solute *i* at equilibrium, kg/m^3
U_f	linear velocity in the positive direction of *z*, m/s
Q_i^*	dimensionless concentration of solute *i* in the solid phase
$\overline{C_i}$	dimensionless concentration of solute *i* in fluid phase of the column
$\overline{X}_i$	dimensionless concentration of solute *i* in pore fluid phase
Z	dimensionless distance

2.3 OBJECTIVE OF THESIS

On the basis of reviewed literature as mentioned above, the following objectives have been planned.

a) To develop the mathematical model for a fixed bed adsorption column for the removal of phenol from waste water.

b) To solve the mathematical model equations by using explicit finite difference technique and by using equation solver like MATLAB.

c) To study the effect of various operating and design parameters on its performance.

Chapter 3

MODEL DEVELOPMENT

3.1 INTRODUCTION

In this chapter, mathematical model have been developed for fixed bed adsorption column. The macroscopic conservation of equation is obtained by applying control volume concept. Control volume is one which encloses certain material entities to which mass balance is applied.

The principle of mass conservation of adsorbate is simply

$$\left\{\begin{array}{l}\text{Rate of accumulation}\\ \text{of adsorbate mass}\\ \text{within control volume}\end{array}\right\} = \left\{\begin{array}{l}\text{Rate of net adsorbate}\\ \text{input into the control}\\ \text{volume associated}\\ \text{with bulk flow}\end{array}\right\} - \left\{\begin{array}{l}\text{Rate of net adsorbate}\\ \text{output into the control}\\ \text{volume associated}\\ \text{with bulk flow}\end{array}\right\}$$

3.2 ASSUMPTIONS

To formulate a generalized model corresponding to the pore diffusion mechanism, following assumptions are made

- The system operates under isothermal conditions.
- The equilibrium of adsorption is described by Langmuir isotherm, a nonlinear isotherm.
- Intra-particle mass transport is due to Fickian diffusion, and it is characterized by the pore diffusion coefficient, D_p.
- Mass transfer across the boundary layer surrounding the solid particles is characterized by the external-film mass transfer coefficient, k_f.
- The linear velocity of the liquid phase varies along the column.
- The macro porous adsorbent particles are spherical and homogeneous in size and density.

3.3 MATHEMATICAL MODELING

The physical process considered in this model. Convection along the column axial direction and axial dispersion are the mass transport mechanisms in the bulk phase. Molecules from the bulk interstitial phase are transported via axial convection and Fickian diffusion (film diffusion) onto the particle surface. Inside the particle, molecules can diffuse into the inner portion of particle via surface diffusion, pore diffusion, or both. This study focuses on understanding the mechanism in pore diffusion.

Based on the preceding assumptions, for the control volume, *A*dz (Figure 3.1), for limiting situation $z \to 0$, net rate of accumulation or depletion is given as [3].

$$-D_L \frac{\partial^2 C_b}{\partial z^2} + V \frac{\partial C_b}{\partial z} + C_b \frac{\partial V}{\partial z} + \frac{\partial C_b}{\partial t} + \rho_P \left(\frac{1-\varepsilon}{\varepsilon} \right) \frac{\partial q_p}{\partial t} = 0 \qquad (3.1)$$

The following initial condition is considered

$$C_b = C_{b0} \qquad z = 0, t = 0 \qquad (3.2)$$

$$C_b = 0 \qquad 0 < z \le L, t = 0 \qquad (3.3)$$

The contour conditions at both ends of the column are given by the following equations

$$D_L \frac{\partial C_b}{\partial z} = -V_0 \left(C_{b0} - C_b \right) \qquad z = 0, t > 0 \qquad (3.4)$$

$$\frac{\partial C_b}{\partial z} = 0 \qquad z = L, t \ge 0 \qquad (3.5)$$

The superficial velocity, V in fixed-bed adsorption is not constant because of adsorption. The following equation was used to estimate (dV/dz), the variation of velocity of bulk fluid along the axial direction of the bed. For liquid adsorption, assuming the liquid density to be constant, then the total mass balance gives

$$\rho_l \frac{\partial V}{\partial z} = -\left(1-\varepsilon\right) \rho_s \frac{\partial q_P}{\partial t} \qquad (3.6)$$

Velocity boundary conditions

$$V = V_0 \qquad z = 0, t > 0 \qquad (3.7)$$

$$\frac{\partial V}{\partial t} = 0 \qquad z = L, t > 0 \qquad (3.8)$$

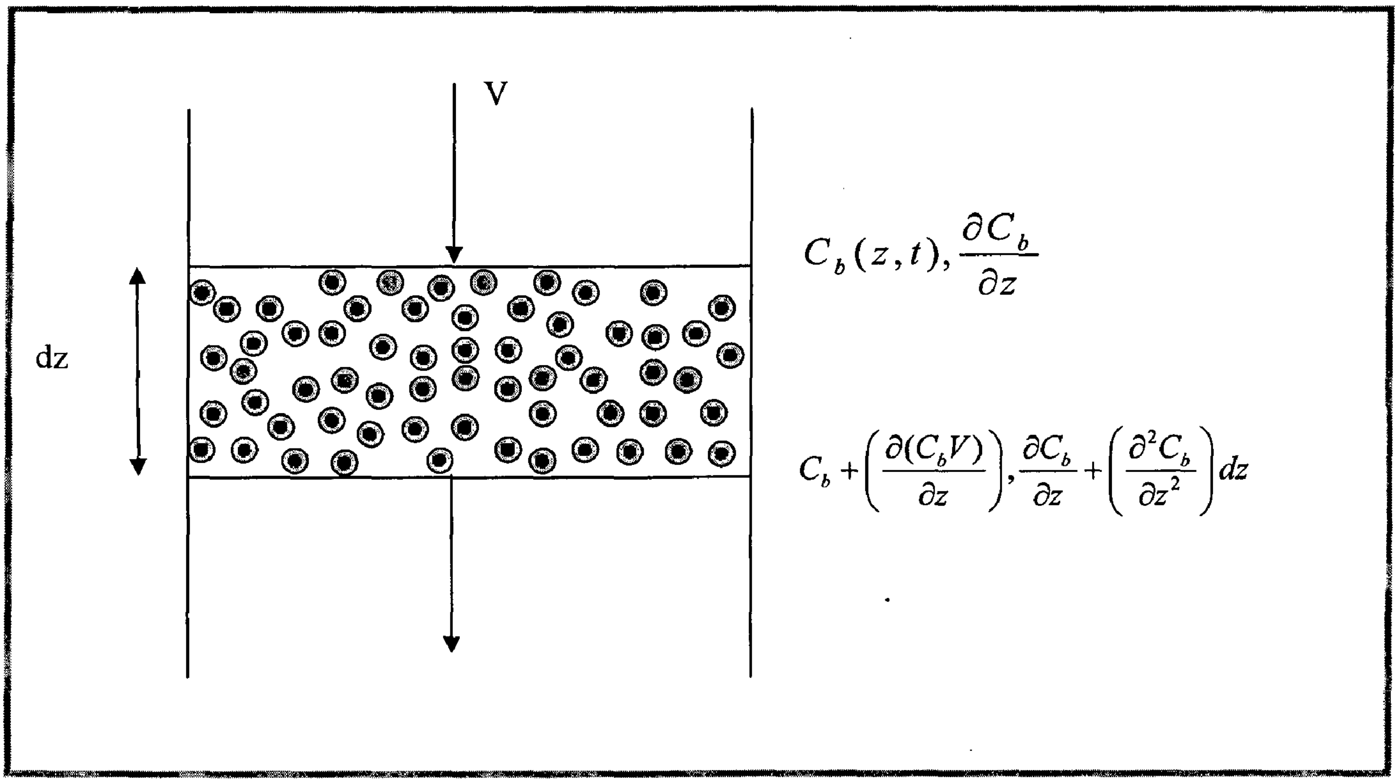

Figure 3.1: Mass balance in element of fixed bed.

The inter-phase mass transfer rate may be expressed as

$$\rho_s \frac{\partial q_P}{\partial t} = \frac{3k_f}{a_P}\left(C_b - C_s\right) \tag{3.9}$$

The intra-pellet mass transfer is due to the diffusion of adsorbate molecules through the pore [3]. The macroscopic conservation equation is given as

$$\varepsilon_P \frac{\partial c}{\partial t} + \left(1-\varepsilon_P\right)\rho_P \frac{\partial q}{\partial t} = D_P\left(\frac{\partial^2 c}{\partial r^2} + \frac{2}{r}\frac{\partial c}{\partial r}\right) \tag{3.10}$$

Assuming instantaneous equilibrium

$$\frac{\partial q}{\partial t} = \frac{\partial c}{\partial t}\frac{\partial q}{\partial c} \tag{3.11}$$

Then rearranging equation

$$\frac{\partial c}{\partial t} = \frac{1}{\left[1 + \rho_P\left(\frac{1-\varepsilon_P}{\varepsilon_P}\right)\frac{\partial q}{\partial c}\right]}\frac{D_P}{\varepsilon_P}\left(\frac{\partial^2 c}{\partial r^2} + \frac{2}{r}\frac{\partial c}{\partial r}\right) \tag{3.12}$$

The following initial condition is considered

$$c = 0, q = 0 \qquad 0 < r < a_P, t = 0 \tag{3.13}$$

The symmetry condition at the center of the particles and continuity condition on the external surface of the adsorbent bed are expressed as

$$\frac{\partial c}{\partial r} = 0 \qquad r = 0, t > 0 \tag{3.14}$$

$$k_f\left(C_b - C_s\right) = D_P \frac{\partial c}{\partial r} \qquad r = a_P, t > 0 \tag{3.15}$$

The adsorption isotherm was favorable and nonlinear, and it described by Langmuir isotherm

$$q = \frac{q_m bc}{1 + bc} \tag{3.16}$$

3.4 NUMERICAL SOLUTION OF MODEL EQUATIONS

The numerical method of solution of the partial differential equations is the method Explicit Finite Difference technique. Since nonlinear adsorption equilibrium is considered, the preceding set of partial differential equations solved numerically by a reduction to set of ordinary differential equations using the Explicit Finite Difference technique.

Equation (3.6) and (3.9) can be written as

$$\frac{\partial V}{\partial z} = -\frac{\rho_s(1-\varepsilon)}{\rho_l}\frac{\partial q_P}{\partial t} \tag{3.17}$$

$$\frac{\partial q_P}{\partial t} = \frac{3k_f}{a_P\rho_s}(C_b - C_s) \tag{3.18}$$

Use equation (3.17) and (3.18) in equation (3.1), we get

$$-D_L\frac{\partial^2 C_b}{\partial z^2} + V\frac{\partial C_b}{\partial z} + \frac{\partial C_b}{\partial t} + \left[\rho_P\left(\frac{1-\varepsilon}{\varepsilon}\right) - C_b\frac{\rho_s}{\rho_l}(1-\varepsilon)\right]\frac{3k_f}{a_p\rho_s}(C_b - C_s) = 0 \tag{3.19}$$

Use equation (3.18) in (3.17), we get

$$\frac{\partial V}{\partial z} = -\frac{\rho_s(1-\varepsilon)}{\rho_l}\left[\frac{3k_f}{a_P\rho_s}(C_b - C_s)\right] \tag{3.20}$$

The Explicit Finite Difference technique is applied by first choosing a new set of dimensionless variables which have values lying between 0 and 1. The following dimensionless variables are defined

$$\overline{C} = \frac{C_b}{C_{bo}}$$

$$Z = \frac{z}{L}$$

$$\tau = \frac{tD_L}{L^2}$$

$$\overline{V} = \frac{V}{V_o}$$

Now using above dimensionless terms in equation (3.19), we get

$$-\frac{D_L C_{bo}}{L^2}\frac{\partial^2 \overline{C}}{\partial \overline{Z}^2}+V_o\overline{V}\frac{C_{bo}}{L}\frac{\partial \overline{C}}{\partial \overline{Z}}+C_{bo}\frac{\partial \overline{C}}{\partial t}+\left[\rho_P\left(\frac{1-\varepsilon}{\varepsilon}\right)-\overline{C}C_{bo}\frac{\rho_s}{\rho_l}(1-\varepsilon)\right]\frac{3k_f C_{bo}}{a_p\rho_s}\left(\overline{C}-\frac{C_s}{C_{bo}}\right)=0$$

$$\frac{\partial \overline{C}}{\partial \tau}=\frac{\partial^2 \overline{C}}{\partial \overline{Z}^2}-\frac{V_o L}{D_L}\overline{V}\frac{\partial \overline{C}}{\partial \overline{Z}}-\left[\frac{\rho_P}{\rho_s}\left(\frac{1-\varepsilon}{\varepsilon}\right)-\frac{C_{bo}}{\rho_l}(1-\varepsilon)\overline{C}\right]\frac{3k_f}{a_p}\frac{L^2}{D_L}\left(\overline{C}-\frac{C_s}{C_{bo}}\right)$$

$$\frac{\partial \overline{C}}{\partial \tau}=\frac{\partial^2 \overline{C}}{\partial \overline{Z}^2}-\alpha\overline{V}\frac{\partial \overline{C}}{\partial \overline{Z}}-\left[\beta-\gamma\overline{C}\right]\psi\left(\overline{C}-\frac{C_s}{C_{bo}}\right) \tag{3.21}$$

where

$$\alpha=\frac{V_o L}{D_L}$$

$$\beta=\frac{\rho_P}{\rho_s}\left(\frac{1-\varepsilon}{\varepsilon}\right)$$

$$\gamma=\frac{C_{bo}}{\rho_l}(1-\varepsilon)$$

$$\psi=\frac{3k_f}{a_p}\frac{L^2}{D_L}$$

Now using above dimensionless terms in equation (3.20), we get

$$\frac{V_o}{L}\frac{\partial \overline{V}}{\partial \overline{Z}}=-\frac{(1-\varepsilon)}{\rho_l}\frac{3k_f}{a_p}C_{b0}\left(\overline{C}-\frac{C_s}{C_{b0}}\right)$$

$$\frac{\partial \overline{V}}{\partial \overline{Z}}=-\frac{(1-\varepsilon)}{\rho_l}\frac{3k_f}{a_p}\frac{L}{V_o}C_{b0}\left(\overline{C}-\frac{C_s}{C_{b0}}\right)$$

$$\frac{\partial \overline{V}}{\partial \overline{Z}}=-\gamma\phi\left(\overline{C}-\frac{C_s}{C_{b0}}\right) \tag{3.22}$$

where

$$\phi=\frac{3k_f}{a_p}\frac{L}{V_o}$$

Transformed initial and boundary conditions are

$$\bar{C} = 0 \qquad \tau = 0 \tag{3.23}$$

$$\frac{\partial \bar{C}}{\partial \bar{Z}} = -\frac{V_0 L}{D_L}\left(1-\bar{C}\right) = -\alpha\left(1-\bar{C}\right), \qquad \bar{Z} = 0 \tag{3.24}$$

$$\frac{\partial \bar{C}}{\partial \bar{Z}} = 0, \qquad \bar{Z} = 1 \tag{3.25}$$

$$\bar{V} = 1, \qquad \bar{Z} = 0 \tag{3.26}$$

The discretization of the equation (3.21) using finite difference scheme gives

$$\left.\frac{\Delta \bar{C}}{\Delta t}\right|_i = \left.\frac{\Delta^2 \bar{C}}{\Delta \bar{Z}^2}\right|_i - \alpha \bar{V} \left.\frac{\Delta \bar{C}}{\Delta \bar{Z}}\right|_i - \left[\beta - \gamma \bar{C}_i\right]\psi\left(\bar{C}_i - \frac{C_s}{C_{bo}}\right)$$

$$\frac{\bar{C}(i,j+1)-\bar{C}(i,j)}{\Delta t} = \frac{\bar{C}(i+1,j)-2\bar{C}(i,j)+\bar{C}(i-1,j)}{\Delta Z^2} - \alpha V(i)\frac{\bar{C}(i+1,j)-\bar{C}(i,j)}{\Delta Z}$$

$$-\left(\beta-\gamma\bar{C}(i,j)\right)\psi\left[\bar{C}(i,j)-\frac{C_s}{C_{bo}}\right] \tag{3.27}$$

Equation (3.22) can be written as

$$\frac{\bar{V}(i+1)-\bar{V}(i)}{\Delta Z} = -\gamma\phi\left(\bar{C}(i,j)-\frac{C_s}{C_{bo}}\right) \tag{3.28}$$

Transformed Initial and Boundary conditions for equation (3.27) becomes

$$\bar{C}(i,1) = 0, \qquad i>1 \tag{3.29}$$

$$\bar{C}(1,j) = 1, \qquad j \ge 1 \tag{3.30}$$

$$\bar{C}(2,j) = \bar{C}(1,j) - \alpha\Delta z\left(1-\bar{C}(1,j)\right), \qquad j \ge 1 \tag{3.31}$$

$$\bar{C}(N,j) = \bar{C}(N-1,j), \qquad j \ge 1 \tag{3.32}$$

Transformed B.C. for equation (3.28) becomes

$$\bar{V}(1) = 1 \tag{3.33}$$

Defining dimensionless variables for equation (3.12)

$$\hat{C} = \frac{c}{C_s}$$

$$\eta = \frac{r}{R}$$

$$\tau = \frac{tD_L}{L^2}$$

Differentiate equation (3.16) and use in equation (3.12)

$$\frac{\partial q}{\partial c} = \left[\frac{q_m b}{(1+bc)^2} \right]$$

$$\frac{\partial c}{\partial t} = \frac{1}{\left[1 + \rho_P \left(\frac{1-\varepsilon_P}{\varepsilon_P} \right) \left[\frac{q_m b}{(1+bc)^2} \right] \right]} \frac{D_P}{\varepsilon_P} \left(\frac{\partial^2 c}{\partial r^2} + \frac{2}{r} \frac{\partial c}{\partial r} \right) \tag{3.34}$$

Use dimensionless term in equation (3.34), we get

$$\frac{\partial \hat{C}}{\partial \tau} = \frac{\left(\frac{D_p L^2}{\varepsilon_p D_L R^2} \right)}{\left[1 + \frac{\rho_p (1-\varepsilon_p) q_m b}{\varepsilon_p (1 + bC_s \hat{C})^2} \right]} \left(\frac{\partial^2 \hat{C}}{\partial \eta^2} + \frac{2}{\eta} \frac{\partial \hat{C}}{\partial \eta} \right) \tag{3.35}$$

$$\omega_1 = \frac{D_p L^2}{\varepsilon_p D_L R^2}$$

$$\omega_2 = \frac{\rho_p (1-\varepsilon_p) q_m b}{\varepsilon_p}$$

Equation (3.35) becomes

$$\frac{\partial \hat{C}}{\partial \tau} = \frac{\omega_1}{\left[1 + \frac{\omega_2}{(1 + bC_s \hat{C})^2} \right]} \left(\frac{\partial^2 \hat{C}}{\partial \eta^2} + \frac{2}{\eta} \frac{\partial \hat{C}}{\partial \eta} \right) \tag{3.36}$$

The Initial and Boundary condition follows

$$\hat{C} = 0 \qquad \tau = 0 \tag{3.37}$$

$$\frac{\partial \hat{C}}{\partial \eta} = 0 \qquad \eta = 0, \tau \geq 0 \tag{3.38}$$

$$\left(\hat{C} - \frac{C_s}{C_{bo}} \right) = \omega_3 \frac{\partial \hat{C}}{\partial \eta} \qquad \eta = 1, \tau > 0 \tag{3.39}$$

The discretization of the equation (3.36) using finite difference scheme gives

$$\left.\frac{\Delta\hat{C}}{\Delta\tau}\right|_i = \left.\frac{\omega_1}{\left[1+\dfrac{\omega_2}{(1+bC_s\hat{C})^2}\right]}\left(\frac{\Delta^2\hat{C}}{\Delta\eta^2}+\frac{2}{\eta}\frac{\Delta\hat{C}}{\Delta\eta}\right)\right|_i \tag{3.40}$$

$$\frac{\hat{C}(i,j+1)-\hat{C}(i,j)}{\Delta\tau} = \frac{\omega_1}{\left(1+\dfrac{\omega_2}{\left(1+bC_s\hat{C}(i,j)\right)^2}\right)}\left\{\left[\frac{\hat{C}(i+1,j)-2\hat{C}(i,j)+\hat{C}(i-1,j)}{\Delta\eta^2}\right]\right.$$

$$\left.+\frac{2}{i\Delta\eta}\left(\frac{\hat{C}(i+1,j)-\hat{C}(i,j)}{\Delta\eta}\right)\right\} \tag{3.41}$$

Transformed Initial and Boundary conditions for equation (3.41) becomes

$$\hat{C}(i,1)=0 \tag{3.42}$$

$$\hat{C}(N,j)=\hat{C}(N-1,j) \tag{3.43}$$

$$\hat{C}(1,j)=1 \tag{3.44}$$

$$\left(\hat{C}(1,j)-\frac{C_s}{C_{bo}}\right)=\omega_3\left(\frac{\hat{C}(2,j)-\hat{C}(1,j)}{\Delta\eta}\right) \tag{3.45}$$

3.5 OPERATING PARAMETERS

In this section various parameters are described which are used in mathematical modeling.

Table 3.1: Parameters used in model equations

Parameters	Value	Unit
Radius of the adsorbent pellets, a_p	3.1×10^{-4}	m
Langmuir isotherm constant, b	0.84	ml/mg
Axial dispersion coefficient, D_L	5.9×10^{-10}	m^2/s
Pore diffusion coefficient, D_p	2.5×10^{-11}	m^2/s
External film mass transfer coefficient, k_f	1.5×10^{-6}	m/s
Column length, L	0.163	m
Maximum adsorption capacity, q_m	45.4	mg/g
Flow rate, Q	0.25	ml/min
Superficial velocity, V	0.0020	m/s
Bed porosity, ε	0.58	---
Porosity of the adsorbent pellet, ε_p	0.53	---
Bed density, ρ_s	900	kg/m^3
Particle density, ρ_p	840	kg/m^3
Inlet concentration, C_{bo}	0.5	mg/ml
Bed diameter, d	0.016	m
Liquid density, ρ_l	1000	kg/m^3

3.6 NUMERICAL SCHEME

Figure 3.2 shows the numerical scheme of explicit finite difference method. This scheme is used in making computer program in MATLAB. Unknown points are calculated from the known points at previous times. On time axis M points are taken and on length axis N points are taken. Intervals should be taken small for proper results.

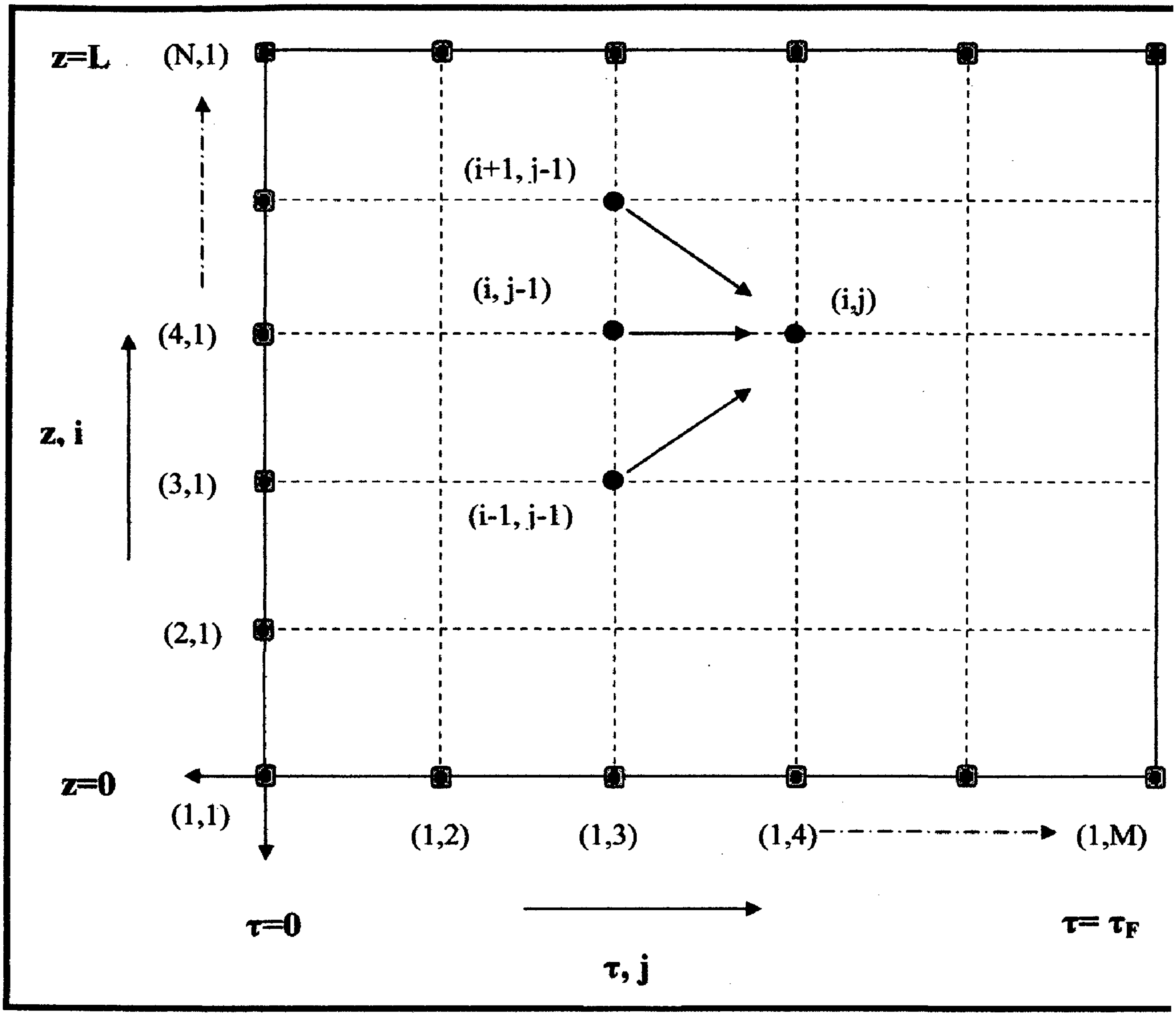

Figure 3.2: Numerical Scheme used in making computer program in MATLAB.

▣	Known points
τ	Time
z	Axial direction
M	Number of points on time axis
N	Number of points on length axis

3.7 SIMULATION TECHNIQUE

Since nonlinear adsorption equilibrium is considered, the preceding set of partial differential equations is solved numerically by using Explicit Finite Difference technique. Final equations along with their initial and boundary conditions are discretized first. The Finite difference technique was then coded in the programming language of MATLAB.

The main inputs to the computer program are:

1. Axial dispersion coefficient.
2. Superficial velocity.
3. Langmuir isotherm constant.
4. Inlet concentration.

The main outputs of computer program are:

1. Adsorption equilibrium data fittings to Langmuir isotherm model.
2. Concentration profile with time which is the break through curve for adsorption column.

Chapter 4

RESULTS AND DISCUSSION

4.1 INTRODUCTION

The present model determines the outlet adsorbate concentration at different times based on different operating conditions. In the present model, linear velocity variation along the bed is considered. Initially the sharp front of the breakthrough curve is seen followed by broadening of tail of the breakthrough curve as shown in Figure 4.1. These obtained results are more justifiable with theoretical phenomena occurring in the adsorption system. The fluid velocity along the bed is a decreasing function of bed length.

The velocity continuously decreases inside the bed with respect to bed length. This phenomenon is validated by the mass balance (Equation 3.6) for velocity variation.

Based on the successful implementation of velocity variation in the model, and supporting evidence in the literature, the simulations are carried out using the present model to carry out a systematic parametric study. The present model is studied by varying the different important parameters such as flow rate, bed height, inlet adsorbate concentration and particle diameter.

4.2 PHENOL CONCENTRATION PROFILE

Initially when waste water is introduced in the bed, at that time bed is fresh and inlet adsorbate concentration is zero (Figure 4.2). But as the time passes the concentration increases. And finally bed will saturate. Initially the phenol concentration is greater which reduces with time.

4.3 EFFECT OF FLOW RATE

The results for different solution flow rates are plotted for a bed height of 0.163 m and an inlet adsorbate concentration of 1 mg/ml (Figure 4.3). The flow rates considered are 0.25, 0.5 and 1.0 ml/min. Figure 4.3 reveals that as the flow rate increases from 0.25 to 1.0 ml/min, the breakthrough curve becomes steeper. This is because of the residence time of the solute in the column, which is not long enough for adsorption equilibrium to be reached at high flow rate. So at high flow rate the adsorbate solution leaves the column before equilibrium occurs. Furthermore, a fixed saturation capacity of bed based on the same driving force gives rise to a shorter time for saturation at higher flow rate. This shows as the flow rate increases the velocity variation effect on breakthrough curve decreases.

4.4 EFFECT OF BED HEIGHT

The effect of bed height on the effluent adsorbate concentration is presented for flow rate of 0.25 ml/min and inlet adsorbate concentration of 1 mg/ml in Figure 4.4. The bed heights considered are 0.163 and 0.20 m. It is observed that as the bed height increases from 0.163 to 0.20 m, the break point time increases with velocity variation along the bed. This shows that at smaller bed height the effluent adsorbate concentration ratio increases more rapidly than for a higher bed height. Furthermore, the bed is saturated in less time for smaller bed heights. Smaller bed height corresponds to less amount of adsorbent. Consequently, a smaller capacity for the bed to adsorb adsorbate from solution and a faster increase in rate of adsorbate adsorption is expected. This shows as the bed height increases the velocity variation effect on breakthrough curve increases.

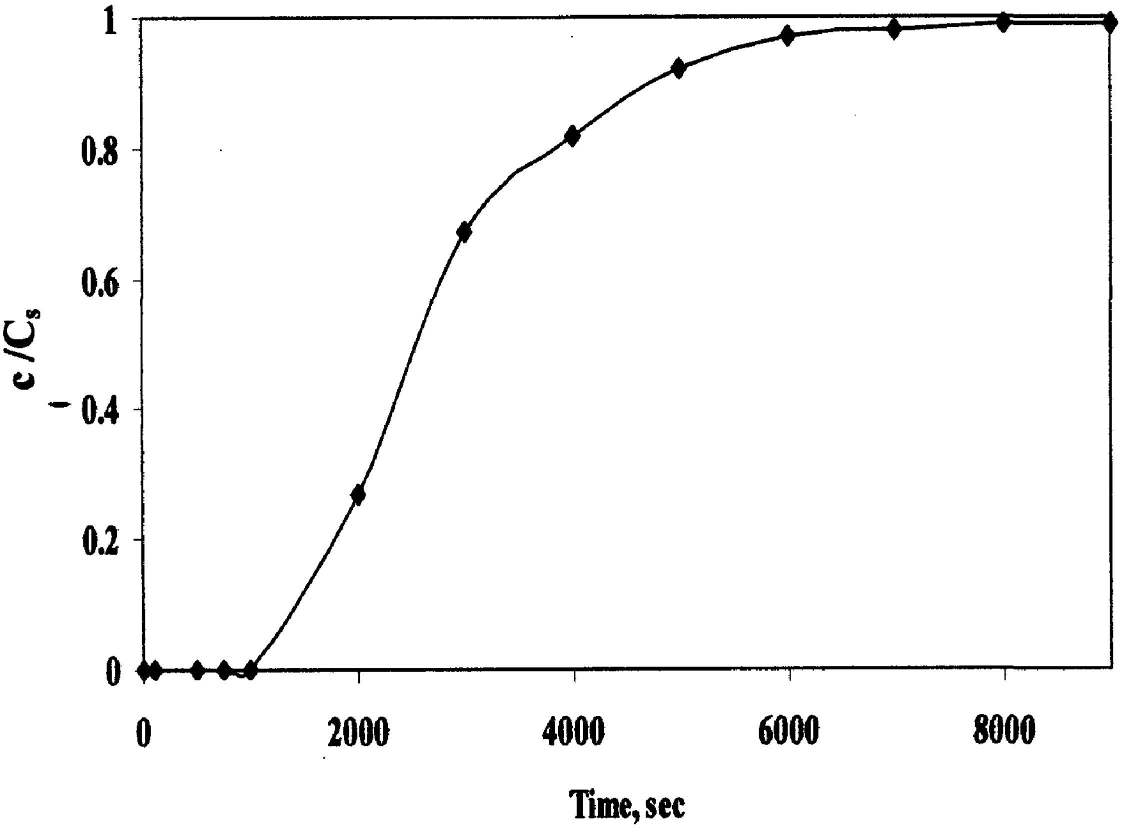

Figure 4.1: Breakthrough curve for the solute concentration with time at V=0.0020 cm/sec.

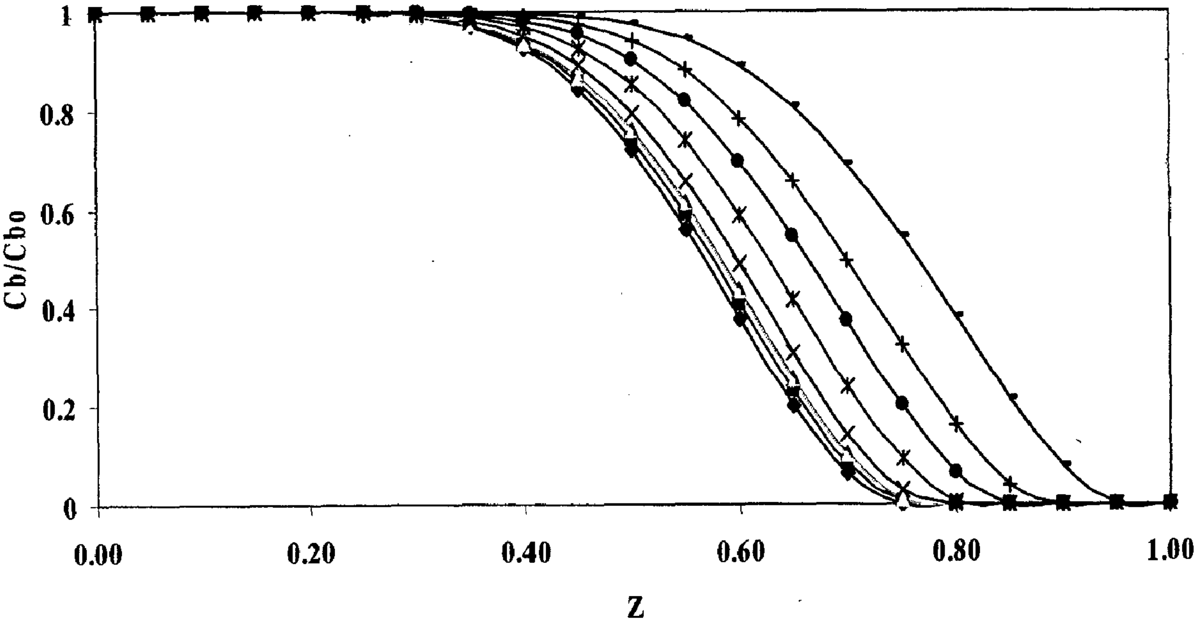

Figure 4.2: Concentration profile along the length of bed as time increases.

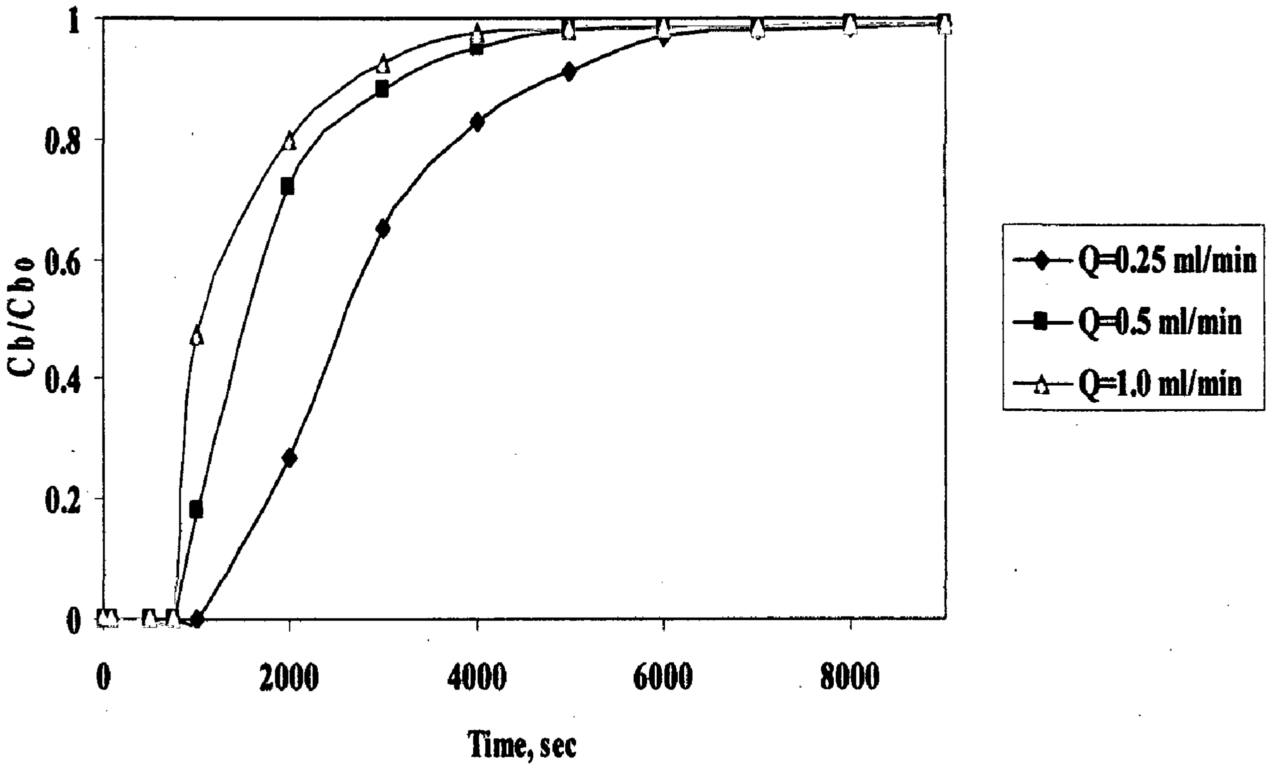

Figure 4.3: Effect of flow rate on breakthrough curve.

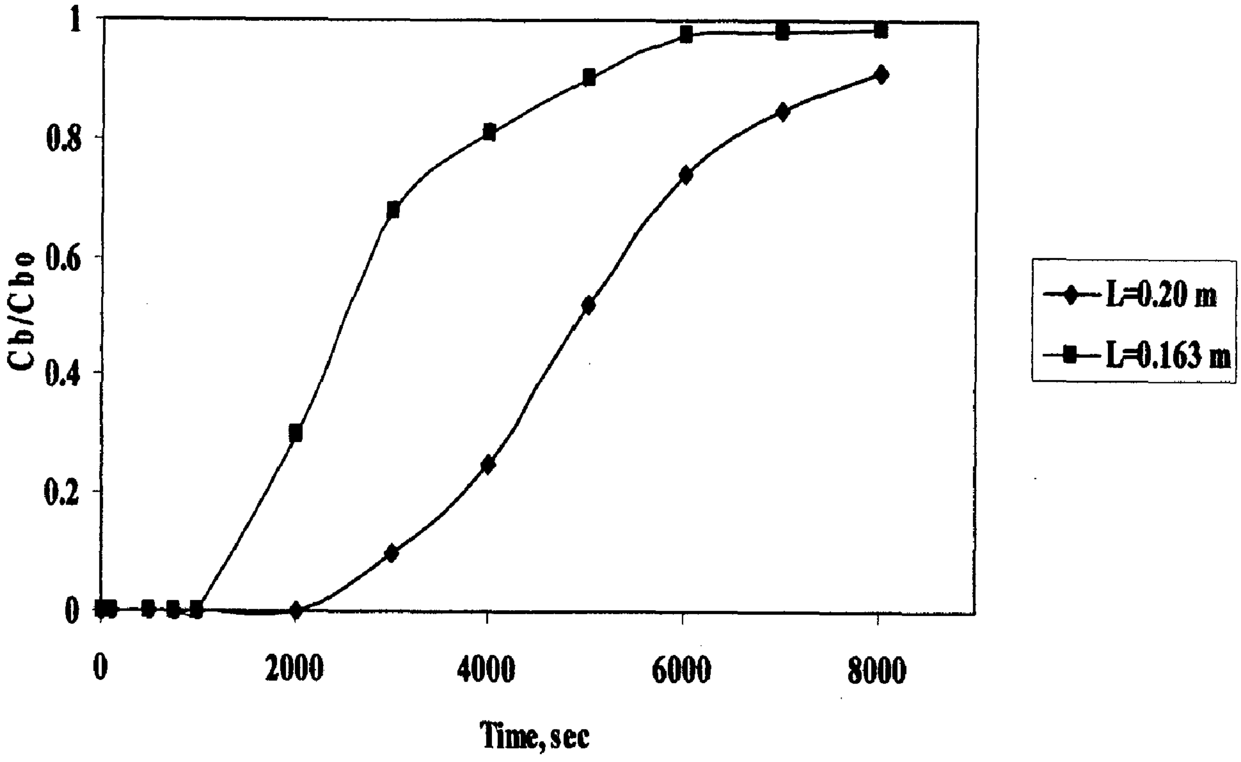

Figure 4.4: Effect of bed height on breakthrough curve.

4.5 EFFECT OF INLET CONCENTRATION

The effect of inlet adsorbate concentration on effluent concentration is shown in Figure 4.5. The two-inlet adsorbate concentrations considered are 0.5 and 1.5 mg/ml. During these simulations other parameters such as bed height and flow rate are kept constant. It is observed that as the inlet adsorbate concentration increases from 0.5 to 1.5 mg/ml, the break point time decreases with velocity variation along the bed. For larger feed concentration, steeper breakthrough curves are found, because of the lower mass-transfer flux from the bulk solution to the particle surface due to the weaker driving force. In addition, at high concentration, the isotherm gradient is lower, yielding a higher driving force along the pores. Thus the equilibrium is attained faster for values of higher adsorbate concentration. This indicates that as the inlet adsorbate concentration increases, there is no significant effect of the velocity variation on breakthrough curve.

4.6 EFFECT OF PARTICLE RADIUS

The effect of particle size on effluent concentration is shown in Figure 4.6. The particle radii considered are 3.1×10^{-4}, 4.1×10^{-4} and 6.1×10^{-4} m. During these simulations other parameters such as flow rate, bed height, and inlet adsorbate concentration are kept constant. Figure 4.6, reveals that as the particle radius increases from 3.1×10^{-4} to 6.1×10^{-4} m, the steepness of the breakthrough curve decreases. The break point time increases with velocity variation along the bed. Smaller particle size resins provide quicker kinetic equilibrium and therefore better breakthrough capacity is obtained at higher linear velocities. This allows faster cycle times with no reduction in the resin capacity. As the diameter of the particle increases, the thickness of stagnant film around the particles increases, and also the total length of the path inside the pores increases. Under these conditions, the overall kinetics of the process is slow, because the time for a molecule of adsorbate to reach the adsorption site is more, as the diffusion path along the pores is large. This shows as the particle radius increases the velocity variation effect on breakthrough curve increases.

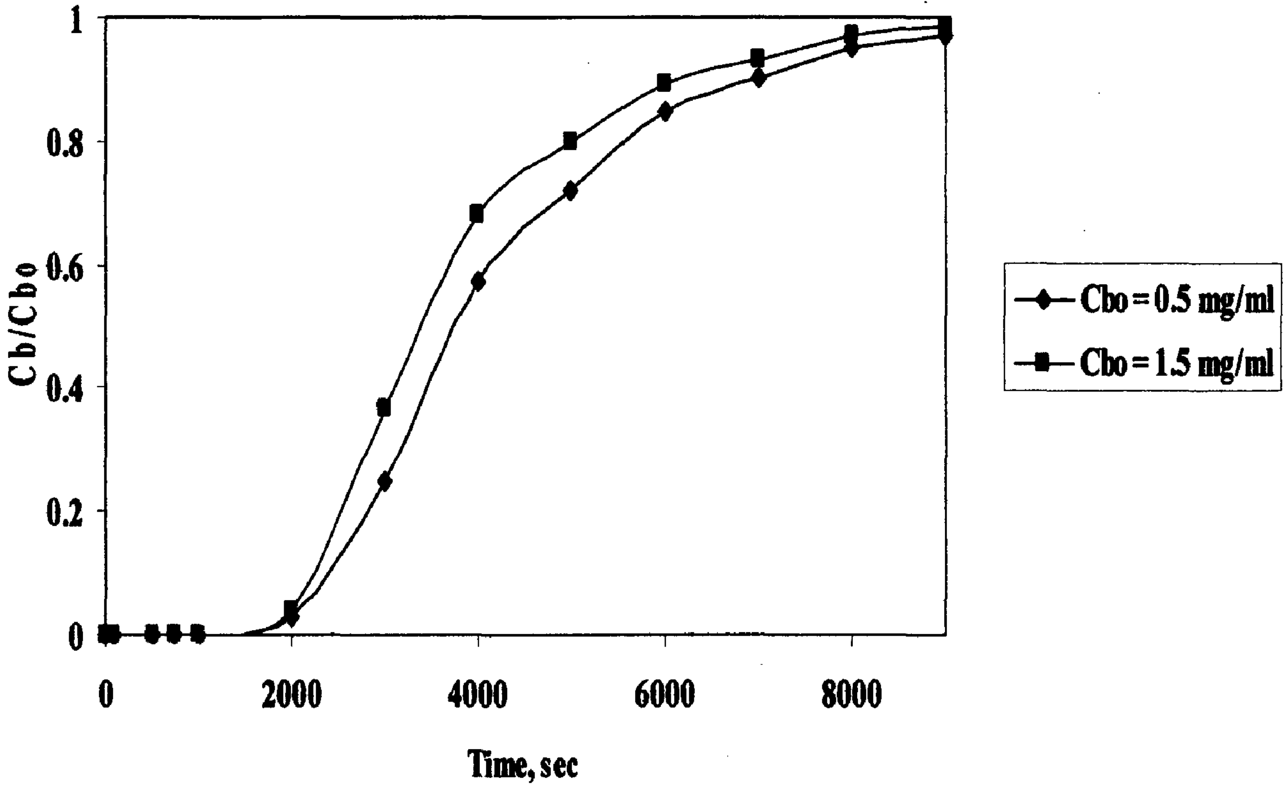

Figure 4.5: Effect of inlet adsorbate concentration on breakthrough curve.

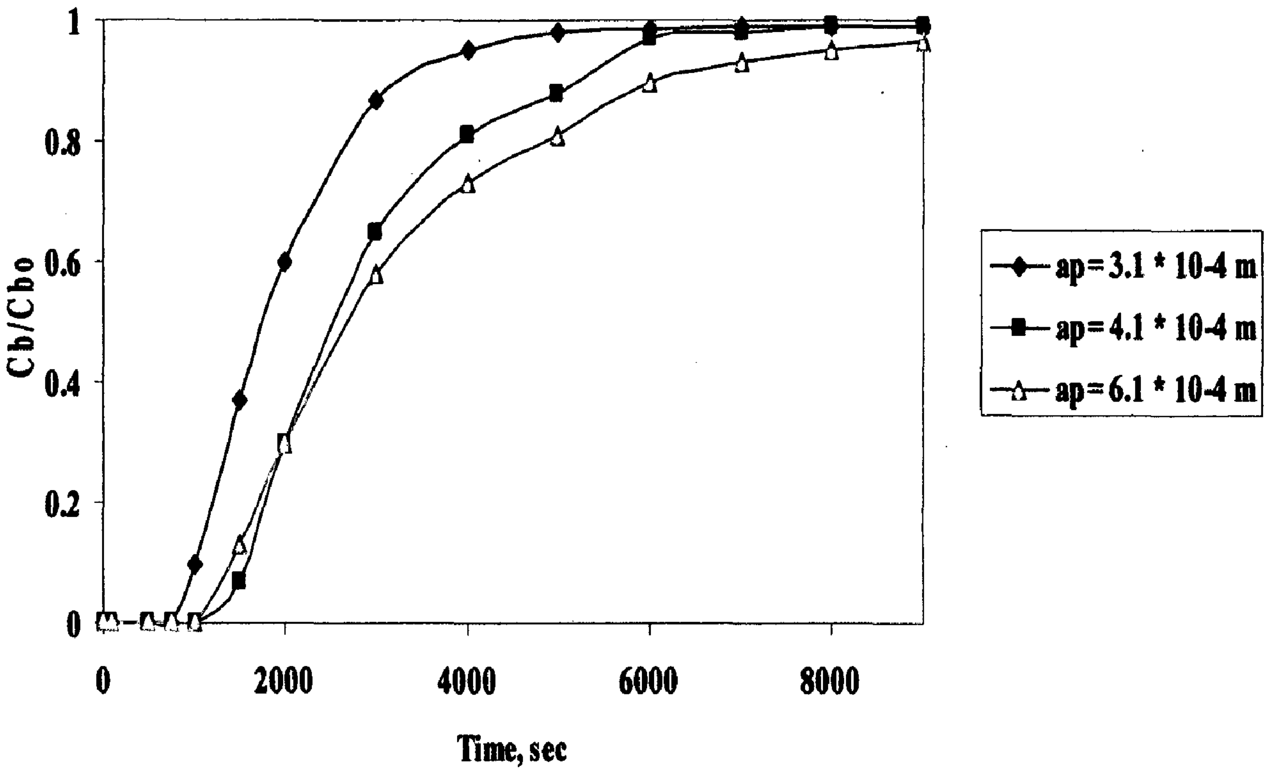

Figure 4.6: Effect of particle radius on breakthrough curve.

Chapter 5

CONCLUSIONS AND RECOMMENDATIONS

5.1 CONCLUSIONS

A generalized model that incorporates external film mass transfer resistance and pore diffusion resistance with velocity variation through column bed has been formulated and solved numerically. Following conclusions are drawn:

1. There is a significant effect of velocity variation through the bed on breakthrough curve, wherein the break point is obtained earlier. Initially the sharp front of the breakthrough curve is seen followed by broadening of tail of the breakthrough curve.
2. As the flow rate is increased, the breakthrough curve becomes steeper. The break point time is obtained earlier and effluent adsorbate concentration ratio increases more rapidly.
3. For smaller bed height, the effluent adsorbate concentration ratio increases more rapidly than for a higher bed height.
4. For larger feed concentration, steeper breakthrough curves are obtained and break point time is achieved sooner.
5. With decrease in particle radius, the breakthrough curve becomes steeper and the break point time decreases.

5.2 RECOMMENDATIONS FOR FUTURE WORK

The research work in the present work could be extended further by the following

1. To study the effect by taking different adsorbents.
2. We can study the adsorption equilibrium data fittings to other isotherm models.
3. To study various models to describe the fixed bed adsorption of phenol.

REFERENCES

[1] **Akarsu, M., H. Sayilkan, S. Sener, F. Sayilkan, E. Arpac**
"Synthesis, Characterization and Applications of Sol-Gel Derived Zirconium Oxide Adsorbent Powder: Removal from Aqueous Solution of Phenol and pChiorophenol"
Turk J. Chem 27 (2003) 477-486.

[2] **Aribike, D. S., O. A. Olafadehan**
"Modeling of Fixed Bed Adsorption of Phenols on Granular Activated Carbon"
Theoretical Foundations of Chemical Engineering 42 (2008) 257-263

[3] **Babu, B. V., Suresh Gupta**
"Modeling and Simulation of Fixed bed Adsorption column: Effect of Velocity Variation"
Journal on Engineering & Technology 1 (2005) 60-66

[4] **Bekkouche, S., M. Bouhelassa, N. H. Salah, F. Z. Meghlaoui**
"Study of adsorption of phenol on titanium oxide ($Ti0_2$)"
Desalination 166 (2004) 355-362.

[5] **Busca, G., S. Berardinelli, C. Resini, L. Arrighi**
"Technologies for the removal of phenol from fluid streams: A short review of recent developments"
Journal of Hazardous Materials 160 (2008) 265-288.

[6] **Costa, C. A. V., A. E. Rodrigues, G. Grevillot, D. Tondeur**
"Purification of phenolic waste water by parametric pumping: Non mixed dead volume Equilibrium model"
AICHE Journal 28 (1982) 73-85.

[7] **Franck, H. G., J. W. Stadelhofer**
"Industrial Aromatic Chemistry"
Berlin: Springer-Verlag, (1988) 148-157.

[8] **Ghiaci, M., A. Abbaspur, R. Kia, F. Seyedeyn-Azad**
"Equilibrium isotherm studies for the sorption of benzene, toluene, and phenol onto organo-zeolites and as- synthesized MCM-41"
Separation and Purification Tech., 40 (2004) 217-229.

[9] **Hameed, B. H., A. A. Rahman**
"Removal of phenol from aqueous solutions by adsorption onto activated carbon prepared from biomass material"
Journal of Hazardous Materials 160 (2008) 576-581.

[10] **Han, Y., X. Quan , S. Chen, H. Zhao, C. Cui, Y. Zhao**
"Electrochemically enhanced adsorption of phenol on activated carbon fibers in basic aqueous solution"
Journal of Colloid and Interface Science 299 (2006) 766-771.

[11] **Kujawski, W., A. Warszawski, W. Ratajczak, T. Porebski, W. Capala, I. Ostrowska**
"Removal of phenol from wastewater by different separation techniques"
Desalination 163 (2004) 286-296.

[12] **Kumar, A. , S. Kumar, S. Kumar**
"Adsorption of resorcinol and catechol on granular activated carbon: Equilibrium and kinetics"
Carbon 41 (2003) 3015-3025.

[13] **Laszlo, K.**
"Adsorption from aqueous phenol and aniline solutions on activated carbons with different surface chemistry"
Colloids and Surfaces A: Physicochemical Eng. Aspects 265 (2005) 32-39.

[14] **Mattson, J. A., J. H. B. Mark, M. D. Malbin, J. W. J Weber, J. C. Crittenden**
"Surface Chemistry of Active Carbon: Specific Adsorption of Phenols"
Journal of Colloid and Interface Science 31 (1969) 116-130.

[15] **Metcalf & Eddy**
Waste water Engineering Treatment Disposal Reuse 4 edition Tata McGraw Hill publishers.

[16] **Mukherjee, S., S. Kumar, A. K. Misra, M. Fan**
"Removal of phenols from water environment by activated carbon, bagasse ash and wood charcoal"
Chemical Engineering Journal 129 (2007) 133-142.

[17] **Nagda, G. K., A. M. Diwan, V. S. Ghole**
"Potential of tendu leaf refuse for phenol removal in aqueous systems"
Applied Ecology and Environmental Res. 5 (2007) 1-9.

[18] **Otero, M., M. Zabkova, A. E. Rodrigues**
"Comparative study of the adsorption of phenol and salicylic acid from aqueous solution onto nonionic polymeric resins"
Separation and Purification Technology 45 (2005) 86-95.

[19] **Otero, M., M. Zabkova, A. E. Rodrigues**
"Adsorptive purification of phenol wastewaters: Experimental basis and operation of a parametric pumping unit"
Chemical Engineering Journal 110 (2005) 101-111.

[20] **Ozkaya, B.**
"Adsorption and desorption of phenol on activated carbon and a comparison of isotherm models"
Journal of Hazardous Materials B129 (2006) 158-163.

[21] **Pan, B. C., F. W. Meng, X. Q. Chen, B. J. Pan, X. T. Li, W. M. Zhang, X. Zhang, J. L. Chen, Q. X. Zhang, Y. Sun**
"Application of an effective method in predicting breakthrough curves of fixed-bed adsorption onto resin adsorbent"
Journal of Hazardous Materials 124 (2005) 74-80.

[22] **Qadeer, R., A. H. Rehan**
"A Study of the Adsorption of Phenol by Activated Carbon from Aqueous Solutions"
Turk J. Chem 26 (2002) 357-361.

[23] **Rengaraj, S., S. H. Moona, R. Sivabalan, B. Arabindoo, V. Murugesan**
"Removal of phenol from aqueous solution and resin manufacturing industry wastewater using an agricultural waste: rubber seed coat"
Journal of Hazardous Materials B89 (2002) 185-196

[24] **Ruthven, D. M.**
Principles of adsorption and adsorption processes, New York John Wiley; 1984.

[25] **Schmidt, R. J.**
"Industrial catalytic processes-phenol production"
Applied Catalysis A: General 280 (2005) 89-103

[26] **Srivastava, V.C., M. M. Swamy, I. D. Mall, B. Prasad, I. M. Mishra**
"Adsorptive removal of phenol by bagasse fly ash and activated carbon: Equilibrium, kinetics and thermodynamics"
Colloids and surfaces A: Physicochem. Eng. Aspects 272 (2006) 89-104.

[27] **Stavropoulos, G. G., P. Samaras, G. P. Sakellaropoulos**
"Effect of activated carbons modification on porosity, surface structure and phenol adsorption"
Journal of Hazardous Materials 151 (2008) 414-421

[28] **Treybal, E. R.**
Mass Transfer Operations 3rd edition, McGraw Hill International editions, Chemical Engineering Series, Singapore.

[29] **Vazquez, G., R. Alonso, S. Freire, G.A. Julia, G. Antorrena**
"Uptake of phenol from aqueous solutions by adsorption in a Pinus pinaster bark packed bed"
Journal of Hazardous Materials B133 (2006) 61-67.